공학석사학위논문

Reusable Nanosorbents Based on Polyethylenimine-Functionalized Magnetite for Removal of Metal Ions from Contaminated Water

가지구조형고분자/자성입자 기반의

재사용이 가능한 수중 중금속 제거용 흡착제에 관한 연구

2014년 2월

서울대학교 대학원

재료공학부

이민영

ABSTRACT

Environmental contamination and human exposure to heavy metals have dramatically increased with growing use in industrial process and products. Some heavy metals are essential to maintain the metabolism of the human body. However, they are serious threats to public health and ecosystem even at low doses due to bioaccumulation. Thus, considerable attention is paid to remove the heavy metal ions efficiently and regenerate the adsorbents from contaminated water.

In this study, we developed the reusable adsorbents for removal of the heavy metal ions such as Cu(II), Pb(II) and As(V) by introduction of b-PEI to magnetite particles. Branched polyethylenimine (b-PEI) is known as a good chelating polymer of the heavy metals. Its amine-rich structures chelate cationic metal ions through electrostatic interaction and are regenerated efficiently with repulsion between protonated amine groups and adsorbed metal. Quaternary ammonium b-PEI also combines with anionic metal ions by ionic-bond interaction and releases the adsorbed anions by ion exchanging. Effectiveness of the magnetite that it is efficiently separated from water in external magnetic field can apply in water treatment process. For removal of Cu(II) and Pb(II), b-PEI functionalized magnetite (P-MG) was synthesized by covalent assembly of

b-PEI to surface of amine-functionalized magnetite (AMG) using a cyanuric chloride as a liking agent. Next, quaternary ammonium polyethylenimine-functionalized magnetite (QP-MG) was prepared by modification of P-MG by glycidyltrimethylammonium chloride (GTA) for removal of anionic metal ions (As(V), Cr(VI)).

The chemical compositions and degree of modification by b-PEI and GTA were investigated using FT-IR spectroscopy, XPS and TGA. It was revealed that b-PEI and quaternary ammonium b-PEI was successfully incorporated in the magnetite. The structure and morphology of adsorbents were characterized by WXRD, FE-SEM and HR-TEM, respectively. It was observed that surface of the adsorbents was covered with organic material such as a polymer. However, all of the adsorbents were maintained the magnetite spheres with spinel structure, so modification using b-PEI and GTA did not affect their morphology and structure. The saturation magnetization of P-MG and QP-MG measured by VSM was similar to that of the AMG, which indicates that the adsorbents have sufficient magnetization (above 60 emu/g) and could be enough to be used for the repeated magnetic separation from water.

To optimization of adsorption and recovery property toward Cu(II), Pb(II), As(V) and Cr(VI), adsorption-desorption experiments were carried out

at various pH conditions. As a result, maximum adsorption efficiencies of the P-MG for Cu(II) and Pb(II) were 96% and 97%. Moreover, it shown high recovery efficiency of more than 94% toward Cu(II) and Pb(II), after 4 recycling test. Especially, adsorption and recovery property of QP-MG were affected with pH conditions because anionic heavy metals have different formation at various pH value in aqueous solution. As a result, maximum recovery efficiency of QP-MG was presented at pH 4.5 toward As(V) and Cr(VI). In the equilibrium isotherm, maximum adsorption capacities of the adsorbents for Cu(II), Pb(II), As(V) and Cr(VI) were estimated 158.7 mg/g, 163.9 mg/g, 20.9 mg/g and 23.5 mg/g by Langmuir model. In additions, adsorption efficiency of the adsorbents was well maintained during the repeated regeneration. The overall results of our studies suggest that P-MG and QP-MG could be used as separable and reusable adsorbents with high efficiency for adsorption of Cu(II), Pb(II), As(V) and Cr(VI) in contaminated water.

Consequently, adsorbents based on b-PEI-functionalized magnetite were successfully prepared and demonstrated to be promising candidates as reusable materials for efficient removal of heavy metal ions in contaminated water.

Keywords

Arsernic; Branched polyethylenimine; Chromium; Heavy metal ions; Magnetic separation; Magnetite; Quaternary ammonium group, Reusable adsorbent, Water treatment

***Student Number*: 2012-20621**

CONTENTS

1. Introduction

Scientific and technological advances relating to water treatment are important in environmental and engineering material research, which has attracted considerable attention for producing safe water throughout the world [1]. With the rapid development of industries and faced with more and more stringent regulations, the excessive and uncontrolled discharge of heavy metal ions becomes one of the most serious environmental and public health problems [2].

Heavy metals are elements having atomic weights between 63.5 and 200.6 and a specific gravity greater than 4.0 (Cr, Co, Ni, Cu, Zn, As, Cd, Sb, Ba, Pb, etc.). Among the toxic metal present in contaminated water, unlike organic contaminants, heavy metals are not degradable and tend to accumulate in living organisms. A number of the heavy metal ions are known to be toxic or carcinogenic at low doses [3]. The heavy metals of particular concern in treatment of industrial wastewaters include copper, lead, arsenics and chromium. Especially, with the broad distribution of unclean water in western China, India, Bangal etc., where the contaminated water usually contains high concentration of toxic copper, lead, arsenics and chromium.

Copper (Cu(II)) is a trace element that is essential for animal metabolism. But the excessive ingestion of copper induces serious toxicological concerns, such as cramps, vomiting, convulsions, or even death. Lead (Pb(II)) can cause central nervous system damage and also damage the kidney, liver, reproductive system and brain functions. The toxic symptoms are anemia, insomnia, dizziness, headache, irritability, weakness of muscles and hallucination [4]. The Cu(II) and Pb(II) form two-electron positive ions in aqueous solution. The cationic heavy metals are found in wastewater coming from manufacturing industries such as a battery, painting, printing, alloy, semiconductor and automobile emissions and mining activities. Therefore, strict regulations have been imposed on the discharge of these heavy metals containing wastewater from industries to decrease negative health effects [5]. As results, examining adsorption conditions of adsorbents toward Cu(II) and Pb(II) would be valuable for removal of cationic heavy metals.

Arsenic also would cause various health problems such as cancer, hypertension, skin diseases and angiocardiopathy [6]. Some of these human health effects are currently being observed in population in Bangladesh, China, India, Mexico and Taiwan where the drinking water is contaminated by arsenic. The WHO (World Health Organization) guideline value for arsenic in drinking water is recommended not to exceed 0.01 mg/L, due to the high toxicity of

arsenics [7]. The arsenic exists two predominant oxyanions in natural surface water, trivalent or pentavalent (As(III), As(V)), both of which are toxic to people and environment [8]. The arsenite (As(III)) is generally regarded to be more toxic. However, the toxicity with different chemical form of arsenic changes as exposed organisms. Such discrepancy may be caused by different pH and redox conditions in the presence of different species, that may related to the degree of water pollution [9]. The As(III) is difficult to separate from water and should be possible only after the oxidation step to As(V). Therefore, the toxicity of As(V) in different surface waters remains still hazardous, and a study examining adsorption conditions of adsorbents as the different chemical form of As(V) in various pH conditions would be valuable to remove As(V) as well as anionic heavy metals. Chromium can exist in two oxidation states, trivalent or hexavalent (Cr(III), Cr(VI)). While Cr(III) is generally non-toxic and is known to stable oxidation state. Also, Cr(III) is believed to be essential element, Cr(VI) is strong oxidizing agents capable of being absorbed through the skin and toxic to animal and plant. Cr(VI) causes skin and stomach irritation at short-term exposure levels above maximum a contaminant. At long-term exposure, it can cause dermatitis, liver, kidney, nerve tissue damage, and even death in large doses. The World Health Organization (WHO) recommended limit for Cr(VI) in drinking water at the level of 0.05 mg/L [10,11,12].

There are many methods to remove heavy metal ions including adsorption, chemical precipitation, ion exchange, membrane filtration and electrochemical treatment.

Adsorption is known to an effective and economic method using activated carbon, chitosan and alumina for heavy metal wastewater treatment. The adsorption process offers flexibility in design and operation, sometimes reversible, adsorbents can be regenerated by suitable desorption process. Chemical precipitation is the most widely used method in industry because it is relatively simple and inexpensive to operate. In precipitation process, chemical react with heavy metal ions to form insoluble precipitates like a hydroxide and sulfide precipitation. The precipitates can be separated from the water by sedimentation or filtration, so it causes secondary waste matter. Ion exchange process using cationic exchanger with carboxylic acid or sulfonic acid group has high treatment capacity, high removal efficiency and fast kinetics. But, it needs high initial cost to install system and is affected by certain variables such as pH, temperature, initial metal concentration and contact time. Membrane filtration such as ultra-filtration, reverse osmosis, nonofiltration and electrodialysis is promising technologies with advantage of high efficiency, easy operation and space saving. However, it requires high cost to operate and cannot avoid a fouling problem [3]. Electrochemical methods involve a

relatively heavy investment and expensive electricity supply, so it hasn't been widely applied [13]. All of the conventional methods have disadvantage of non-reusable, so we need for development of reusable and separable nanosorbents for efficient removal of metal ions from contaminated water.

In recent years, many researchers have been focused on the development of adsorbents, which is modified using nanomaterials with a number of functional group such as a polymer [14]. Branched polyethylenimine (b-PEI) well-known cationic polymer with high contents of amino groups enables in different field of application, e.g. as flocculation aid in paper industry, delivery of gene in biochemistry and as a chelating agent for metal ions in waste water treatment [15,16]. The effectiveness of b-PEI in these applications is attributed to its amine-rich structure (primary, secondary and tertiary amine) in shown Figure 1. Various functional groups including carboxylate, hydroxyl, sulfate, phosphate, amide and amino groups, have been found to be responsible for metal adsorption. Among these, amine group is the most effective functional group for removal of heavy metals. It chelates cationic metal ions as well as adsorbs anionic metal species through electrostatic interaction or hydrogen bonding [17]. Such an electrostatic interaction between adsorbents and metal ions plays an important role in the process of adsorption and desorption. Hence, b-PEI, which is composed of plenty of amine groups in macromolecule chains,

exhibits strong adsorption ability to remove the heavy metals [18]. In addition, advantage of the b-PEI is water soluble, highly branched structure, resistance of aggregation of nanoparticles and feasible for surface modification by different functional groups. To further promote adsorption property toward anionic metal ions, modifications involving alkylation or quaternization using methyl iodide, benzyl chloride, quaternary ammonium epoxide, and glycidyltrimethyl-ammonium chloride have been investigated by large number of researchers [18,19]. Positive charge of quaternary ammonium groups in modified b-PEI interacts with metal anions such as arsenics and chromate.

The b-PEI combines with heavy metal ions through chelating interaction between amine groups of polymer chains and two-electron positive ions at neutral and alkaline conditions. At acidic conditions, it release for adsorbed metal cations from b-PEI by electrostatic repulsion between protonated amine groups and positive metal ions (see Figure 2). The quaternary ammonium b-PEI interacts with anionic metal ions by ionic-bond interaction between positive charged quaternary ammonium groups of polymer and metal anions at various pH. At alkaline or acidic conditions, it regenerated through ion exchanging by H^+ and OH^-, and the result in desorption of the adsorbed metal anions (see Figure 3).

For application in the water treatment, required characteristics of

polymer are the purity and identity. Most of b-PEI is already commercially available and it is commonly believed that the molecular weight between 5 and 25 kDa is most suitable for interior of the body because higher molecular weights lead to increasing of cytotoxicity [15,16]. Thus, b-PEI is promising nanomaterials to remove the heavy metals and release the adsorbed metal ions efficiently from polymer.

With the increasing demand for economical water treatments, the development of novel, low-cost, robust, efficient and reusable adsorbents remains a significant challenge [14]. The magnetic particles have been a considerable subject because of their great potential applications in magnetic fluids, catalysis, biotechnology, magnetic resonance imaging and purification of environmental area by adsorption. Especially, the use of micro- and nanoscale magnetic particles for heavy metal remediation has been increased in recent past, because it is easily separated and reused from water treatment process, which is economical, saving the resources and secondary contaminants. The characteristics of magnetic particles in these applications are attributed to its non-toxic, abundant deposits, paramagnetism and facile synthesis method by solvent thermal reaction. In addition, a number of researchers have been investigated to development of spherical magnetite (Fe_3O_4) aggregates through a simple solvo-thermal process. However, magnetic nanoparticles (~10 nm)

tend to aggregate into bulky particles, which resulting a significant decreasing in adsorption capacity. For nanosized magnetic particles (smaller than 100 nm), the randomly directed forces of Brownian motion are stronger than the magnetic forces and thus result in individual nanoparticles cannot be effectively separated in a moderate magnetic field. Such disadvantage causes that strength of employing magnetic fields and the cost of processing are increased. Consequently, how to develop magnetite adsorbents of high capacity and efficient separation becomes interesting and challenging topic in the field of environmentally functional materials [20].

Many researchers have been modified surface of the magnetite using polymer, reagents with functional groups to reduce the aggregation, and thus result in increasing of dispersibility and efficient separation from contaminated water at moderate magnetic field. Amine-functionalized magnetite is stable in water, suppression of agglomeration and possible to modify the surface by various functional groups. Besides, fabrication of modified magnetite particles could improve for removal of the heavy metals through attachment of a functional polymer such a b-PEI on the surface amine-functionalized magnetite.

In the present study, to development of reusable adsorbents for efficient removal of metal ions, we aim to synthesis of polyethylenimine functionalized magnetite (P-MG) and quaternary ammonium polyethylenimine-

functionalized magnetite (QP-MG). There are three steps to synthesis of P-MG for adsorption toward cationic heavy metal (Cu(II), Pb(II)). First, amine-functionalized magnetite (AMG) spheres are obtained using one-pot synthesis by solvo-thermal treatment [21]. Second, amine groups on the surface of AMG are modified with cyanuric chloride in ice bath [22]. The cyanuric chloride is used as a linking agent to form covalent-bond between AMG and b-PEI, and then we successfully synthesize P-MG. Fundamental information such as molecular weights and degree of the branching related to the b-PEI was obtained using C^{13} NMR and FT-IR analysis. Finally, quaternization is achieved to make positive charged quaternary ammonium groups on the P-MG using glycidyltrimethylammonium chloride (GTA) [23]. Successful synthesized QP-MG would combine with anionic metal ions (As(V), Cr(VI)).

The objective of this work was to discuss the development of reusable adsorbents containing b-PEI and quaternary ammonium functionalized b-PEI for removal of metal ions from contaminated water. Moreover, applicability of prepared adsorbents is investigated through the experiment for evaluation of adsorption and recovery properties. The structural features and morphology of the AMG were characterized by wide angle X-ray diffractometer (WXRD), high-resolution transmission electron microscopy (HR-TEM) and field-emission scanning electron microscopy (FE-SEM). The b-PEI introduced in P-

MG was analyzed qualitatively using fourier transform infrared (FT-IR) spectroscopy, elemental analysis (EA) and X-ray photoelectron spectroscopy (XPS). The amount of b-PEI incorporated in magnetic particles was measured by thermogravimetric analysis (TGA).

The quaternary ammonium groups of b-PEI combined with the magnetic particles was analyzed qualitatively and quantitatively using wide angle X-ray diffractometer (WXRD), high-resolution transmission electron microscopy (HR-TEM), field-emission scanning electron microscopy (FE-SEM), fourier transform infrared (FT-IR) spectroscopy, X-ray photoelectron spectroscopy (XPS) and thermogravimetric analysis (TGA). After surface modification, it was characterized that the structure and morphology of adsorbents were retained with original phase of magnetite spheres by X-ray (XRD), high resolution (HR-TEM) and field-emission scanning electron microscopy (FE-SEM). The results that AMG, P-MG and QP-MG were maintained the enough magnetization to efficient separation and recovery from water were confirmed using vibrating sample magnetometry (VSM). The adsorption and recovery properties of the prepared adsorbents toward heavy metal ions (Cu(II), Pb(II), As(V) and Cr(VI)) were investigated by adsorption-desorption process at various pH value. The concentrations of the solution at before and after the adsorption were evaluated by inductively coupled plasma-

atomic emission spectroscopy (ICP-AES) to confirm capacity of adsorbed metal ions. In additions, recovery efficiency of the adsorbents was measured by releasing of the metal ions from adsorbents.

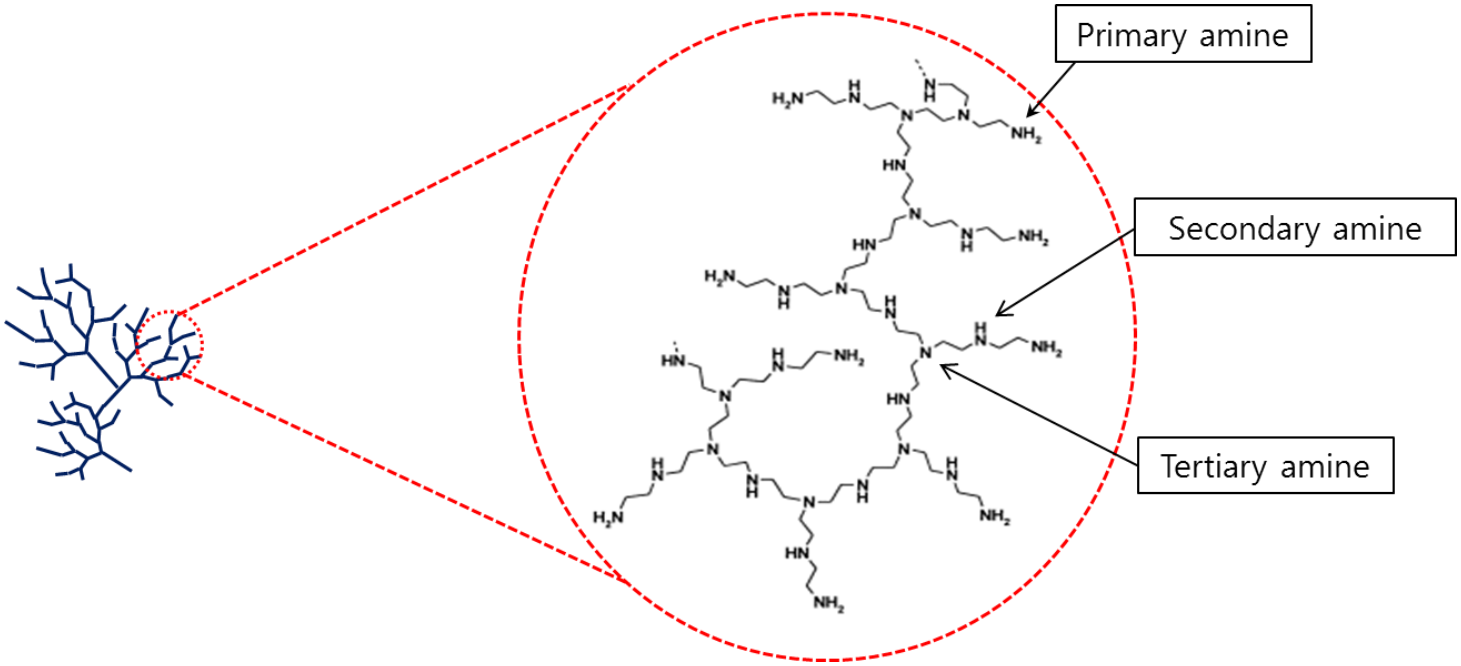

Figure 1. Amine-rich structure of b-PEI

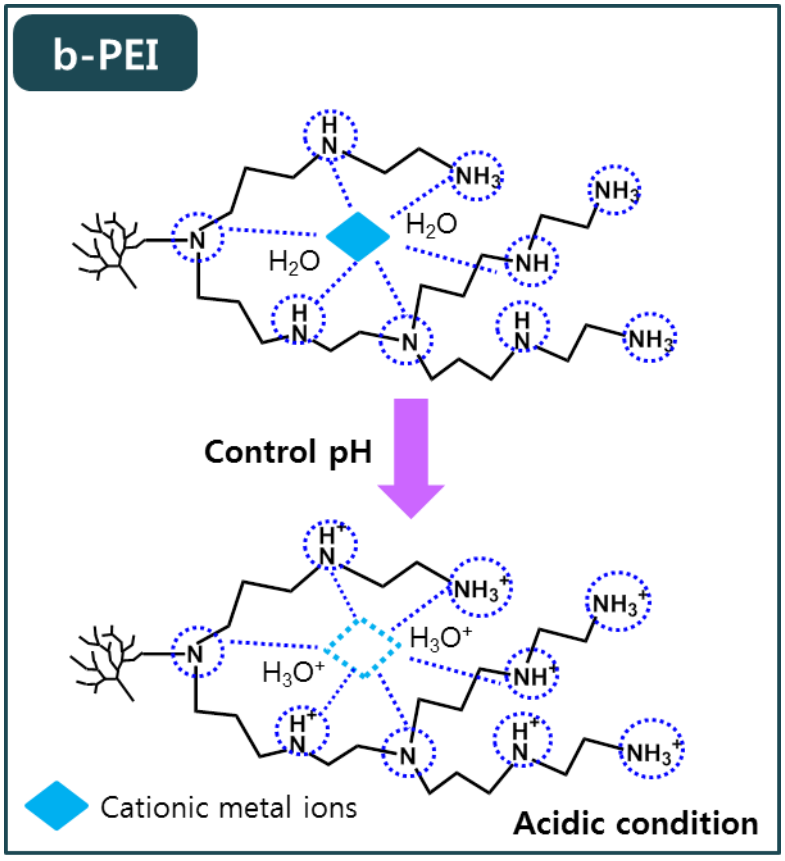

Figure 2. Adsorption and desorption mechanisms of b-PEI

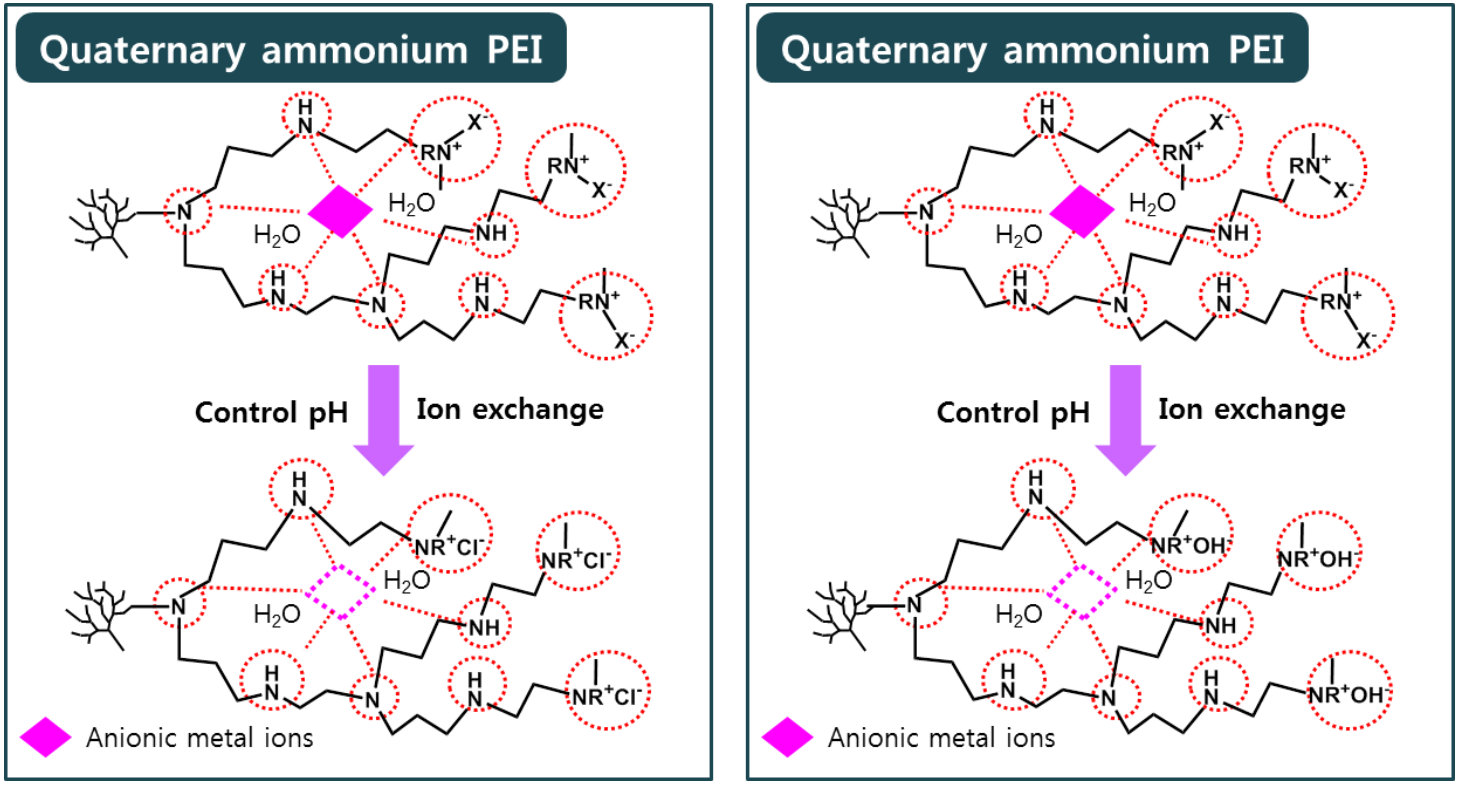

Figure 3. Adsorption and desorption mechanisms of quaternary ammonium b-PEI; (a) Acidic conditions (b) Alkaline conditions

2. Experimental Section

2.1. Materials

Anhydrous sodium acetate, ethylene glycol, iron(Ⅲ) chloride hexahydrate ($FeCl_3 \cdot 6H_2O$), 1,6-diaminohexane, cyanuric chloride, glycidyltrimethyl ammonium chloride, dimethylformamide and polyethylenimine (b-PEI, branched, M_w=25,000) were purchased from Sigma Aldrich (St. Louis, MO, USA) and were used without further purification. The metal ions adsorption properties were tested using copper nitrate trihydrate ($Cu(NO_3)_2 \cdot 3H_2O$), lead nitrate ($Pb(NO_3)_2$), sodium arsenate dibasic heptahydrate ($Na_2HAsO_4 \cdot 7H_2O$) and potassium dichromate ($K_2Cr_2O_7$) were purchased from Sigma-Aldrich. All other chemicals (0.1 N, 1 N NaOH standard solution and 0.1 N, 1 N HCl standard solution etc.) were purchased from Daejung chemical Co., Ltd and were of reagents grade. The water used in all syntheses and tests were distilled and deionized.

2.2. Preparation of polyethylenimine-functionalized magnetite (P-MG)

2.2.1. Synthesis of amine-functionalized magnetite (AMG)

The amine-functionalized magnetite spheres were prepared by the modified hydrothermal method described previously (see Figure 4) [21]. First, anhydrous sodium acetate (2.0 g) dissolved in ethylene glycol (30 mL) at room temperature to give a transparent solution. To this solution were added $FeCl_3 \cdot 6H_2O$ (1.0 g) as ferric sources and 1,6-hexadiamine (6.5 g), followed by vigorous stirring at 50 ℃ for at least 2 h. This solution was transferred into a teflon-lined autoclave and reacted at 198 ℃ for 6 h, and allowed to cool down to room temperature. The product were washed several times with water and ethanol to remove the solvent and unbound 1,6-diaminohexane effectively. During each washing step, the products were separated from the mixtures by using magnetic force. Finally, the materials dried in vacuum oven at 50 ℃ for 12 h to gain the black powder. The prepared sample was designed AMG.

2.2.2. Preparation of P-MG

The preparation of polyethylenimine-functionalized magnetite was included two steps. The first step was carried out in order to modify the amine

group of AMG. Before introducing of branched polyethylenimine (b-PEI) on the surface of AMG, the materials were modified by cyanuric chloride (see Figure 5) [22]. First, AMG (0.1 g) was placed in a three-necked flask containing acetone (250 mL) and stirred to disperse for several minutes. Subsequently, cyanuric chloride (4.6 g) was added to this mixture, which was allowed to react in an ice water bath for 3 h. During the reaction, 1 N NaOH was added drop-wise into the mixture to neutralize the HCl released until the pH was adjusted to 6.0-6.5. The products were rinsed several times (2 or 3 times) with water and ethanol to remove the unbound cyanuric chloride, and then dried in vacuum oven at 50 ℃ for 12 h.

The second step was performed to introduce the b-PEI on surface of the intermediate product from the first step (see Figure 6). The intermediate product (50 mg) was dispersed in distilled water (50 mL) and 0.1 N NaOH (20 mL). A homogeneous solution of b-PEI was made up by adding b-PEI (4 g) into distilled water (50 mL) and then was added into the mixture. The suspension was ultrasonicated at room temperature for 10 minutes, and then the flask was connected to evaporator. After heating for 1 h at 60 ℃, 1 h at 80 ℃, 1 h at 100 ℃ under reduced pressure, the product was obtained.

The resulting particles were washed with distilled water followed by ethanol. After drying in a vacuum oven overnight at 50 ℃, the product was

gained the black powder. The prepared sample was designed P-MG.

2.3. Synthesis of quaternary ammonium polyethylenimine-functionalized magnetite (QP-MG)

The quaternary ammonium polyethylenimine-functionalized magnetite was prepared by dispersing P-MG (50 mg) indimethylformamide (DMF) /distilled water mixture (1:1, v/v) using a three-neck flask. After stirring for a few minutes, glycidyltrimethylammonium chloride (GTA, 25 mL) was added drop-wise into the flask and heated at 60 ℃ for 24 h. The product was washed with distilled water and methanol to effectively remove the byproducts, and then dried in a vacuum oven at 50 ℃ for 12 h. This resulting particles, prepared sample was designed QP-MG (see Figure 7).

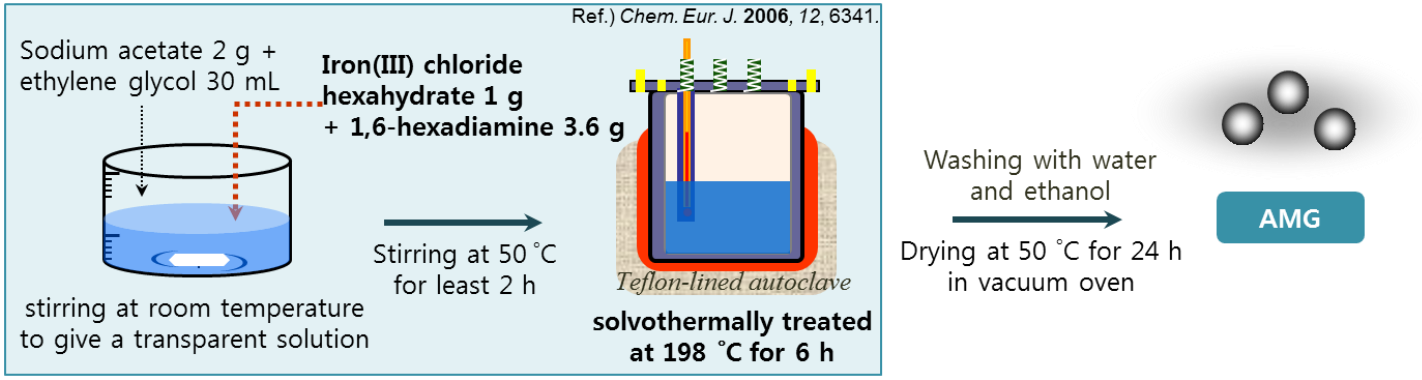

Figure 4. Synthesis of AMG

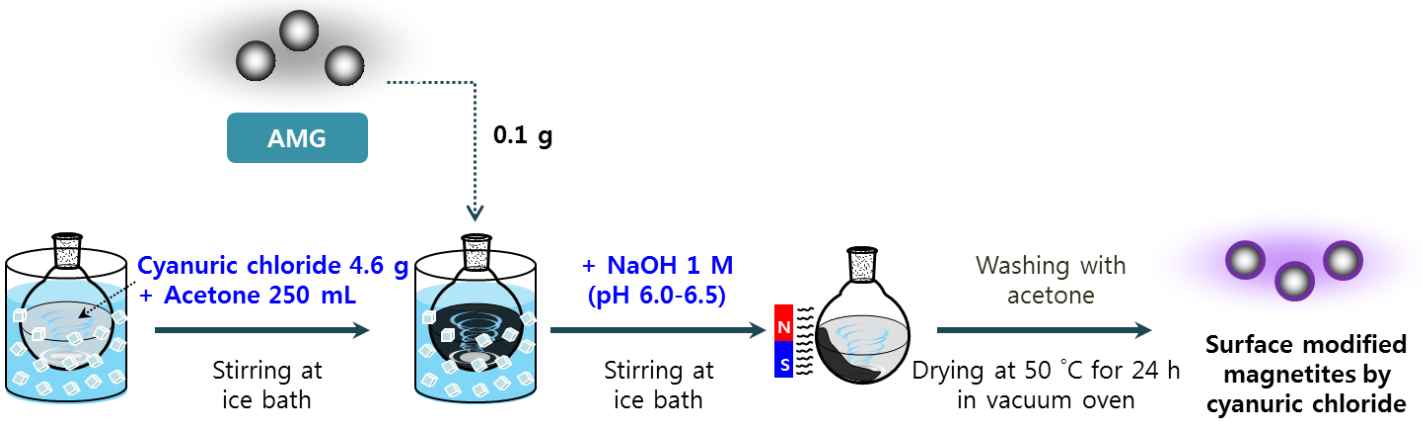

Figure 5. Synthesis of surface modified magnetic particles by cyanuric chloride

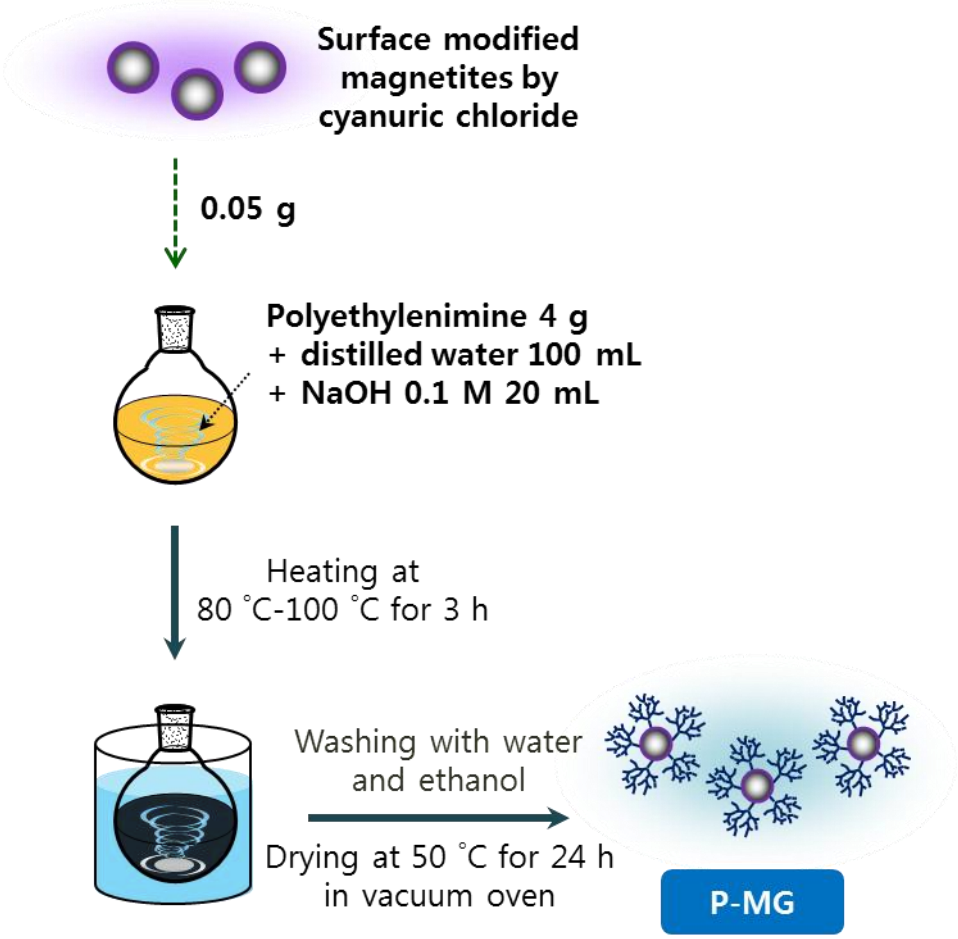

Figure 6. Synthesis of P-MG

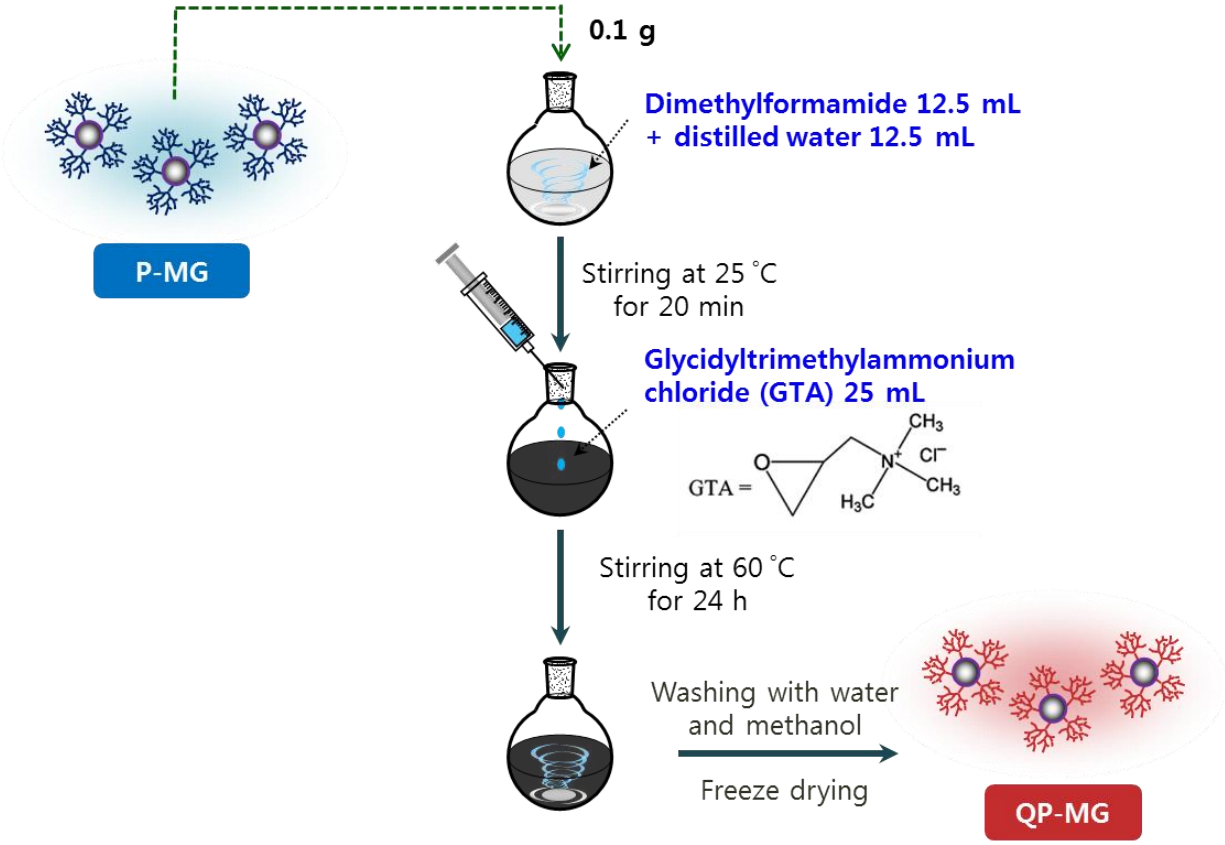

Figure 7. Synthesis of QP-MG

2.4. Characterization of P-MG and QP-MG

2.4.1. Characterization of branched polyethylenimine (b-PEI)

The polymer used in this study is commercial b-PEI (Sigma Aldrich) with a reported M_w=25,000. We analyzed quantitatively specific stretching and bending vibrations of the b-PEI using FT-IR. The FT-IR spectra was collected on samples palletized with KBr powders over the range 4000-400 cm^{-1} with a spectral resolution of 4 cm^{-1} using a Thermo Scientific Nicolet iS10 IR spectrophotometer. The b-PEI was analyzed by C^{13} Nuclear magnetic resonance (NMR) spectra to confirm the structures of b-PEI. The spectrum was recorded on a Bruker AVANCE 600 spectrometer with D_2O used as solvent. The b-PEI solution was prepared in H_2O or D_2O at 10 % (w/v) and characterized using C^{13} inverse gated NMR at 333 K to calculate for degree of branching (DB) in the polymer. The DB defines as

$$\mathrm{DB}=\frac{2D}{(2D+L)}$$

(D= dendritic units, L= linear units).

2.4.2. Characterization of P-MG and QP-MG

The physicochemical properties of the adsorbents were characterized using a broad range of analytical tools including WXRD, HR-TEM, FE-SEM, VSM, FT-IR spectroscopy, EA, XPS, TGA and ICP. Crystal structure and morphology of adsorbents were characterized using a WXRD, HR-TEM and SEM. The WXRD patterns of each sample were collected at room temperature using a MAC/Sci MXP 18XHF–22SRA diffractometer equipped with graphite monochromatized Cu Ka radiation (λ = 1.541 Å, 50 kV, 100 mA) as the X-ray source. The step scans were recorded for 2θ values over the angular range of 15–80° with a scanning speed of 5° min^{-1}. The average crystal diameter was calculated according to the *Debye-Scherrer's formula*, $D = K\lambda/\beta\cos\theta$, where D is the crystallite size, K (= 0.89) is a constant related to the shape of the crystal, λ is the wavelength of the radiation employed, b is the obtained peak width (full width at half maximum, FWHM) in radians, and θ is the Bragg diffraction angle. The morphology of the material was examined using a JEOL JEM-2000EXII high-resolution TEM (HR-TEM) with an operated at an accelerating voltage of 200 kV. The images of magnetic particles were obtained on a Carl Zeiss SUPRA 55VP FE-SEM with an applied voltage of 3.0 kV and equipped with an energy-dispersive spectroscopy (EDS) detector to determine the composition.

Magnetization of each sample was measured in the solid state at room temperature using a vibrating sample magnetometry (VSM). The hysteresis loops for each sample were measured at 300 K in a magnetic field in the range of ±10 kOe. The qualitative and quantitative analysis of introduced b-PEI on adsorbents was performed using a FT-IR spectroscopy, EA, XPS and TGA. FT-IR spectra was collected on samples palletized with KBr powders over the range 4000–400 cm^{-1} with a spectral resolution of 4 cm^{-1} using a Thermo Scientific Nicolet iS10 IR spectrophotometer. The elemental analysis (EA) was measured on a Flash 2000 (CE Instrument, Italy). X-ray photoelectron spectroscopy (XPS) was carried out on a KRATOS AXIS photoelectron spectrometer at background pressure of about 1.0×10^{-9} Torr using Mg Ka X-rays as the excitation source (1253.6 eV). All binding energies were calibrated relative to the C 1*s* peak at 284.5 eV. TGA was determined on a TA Instruments Q500 and the temperature was varied over 25–600 ℃ with a scan rate of 10 ℃ min^{-1} under a stream of nitrogen.

2.5. Evaluation of adsorption and recovery property of P-MG and QP-MG

2.5.1. Adsorption and recovery property of P-MG toward Cu(II) and Pb(II)

A series of heavy metal adsorption studies was conducted for investigation of pH, adsorption efficiency, adsorption isotherm and regeneration. The stock solutions (1 L) of heavy metal were prepared in glass bottles containing $Cu(NO_3)_2 \cdot 3H_2O$ (10 mg) and $Pb(NO_3)_2$ (10 mg), respectively. All batch experiments were conducted in glass vials (70 mL) containing heavy metal ions of the stock solutions. Adsorption studies were conducted at various pH conditions to determine the maximum adsorption efficiency of heavy metal ion (Cu^{2+}).

Representative conditions of the adsorption and desorption are summarized in Table1. Typically, P-MG (10 mg) was added to the stock solution (50 mL) containing each heavy metal ions. The mixture was adjusted pH by a 0.1 N NaOH solution to pH 8.0±0.1. The mixture was dispersed using constant temperature incubator shaker at 25℃ for 2 h. Separation of the P-MG adsorbed heavy metal ions was completed in a few minutes applying external magnet. The concentration of residual heavy metal ions in solution was measured by inductively coupled plasma atomic emission spectroscopy (ICP-

AES). The adsorption efficiency, A% of the heavy metal ions was calculated according to

$$A\% = \frac{(C_i - C_e)}{C_i} \times 100$$

,where C_i (mg L^{-1}) is the initial concentration of heavy metal ions, C_e (mg L^{-1}) is the residual concentration of heavy metal ions. In all the experiments, each test was conducted in duplicates and the data was reported as mean values. In order to assume the maximum adsorption capacity of the P-MG for heavy metal ions, the equilibrium adsorption isotherm experiments were carried out for various concentrations of heavy metal ions. Stock solution of heavy metal ions was prepared in glass bottles containing $Cu(NO_3)_2 \cdot 3H_2O$ from 10 mg/L to 400 mg/L and $Pb(NO_3)_2$ from10 mg/L to 200 mg/L, respectively. Regeneration studies were performed by dispersing used P-MG in to distilled water (50 mL) and the solution was controlled pH by a 1 N HCl solution to pH 2.0±0.1. Then adsorbents were washed repeatedly with excess amounts of distilled water. The procedure was the same as the above with no exception.

The recovery efficiency, R% was determined following equation:

$$R\% = \frac{Q_r}{Q_i} \times 100$$

,where Q_i is the uptake of heavy metal ions and Q_r is the uptake of heavy metal ions after the regeneration procedure. The recovery system is illustrated in detail in Figure 8.

2.5.2. Adsorption and recovery propertyof QP-MG toward As(V) and Cr(VI)

A stock arsenic solution was prepared with $Na_2HAsO_4 \cdot 7H_2O$ (10 mg) in distilled water (1 L). All batch sorption tests were conducted in glass vials, which are contained the prepared stock arsenic solution (50 mL). Representative conditions for the adsorption and desorption are summarized in Table 2 and Figure 9. A little adsorbent (10 mg) was added to a vial, and then the solution was adjusted using a 0.1 N NaOH solution to pH 4.5, 6.0, 8.0±0.1. The mixture was shaken in a thermostatic shaker at 25℃ for 2 h, and then QP-MG adsorbed arsenate was separated at magnetic field. The arsenate adsorption efficiency, A% was calculated above the same equation using ICP. The equilibrium studies for assuming the maximum capacities of As(V) were carried

out by agitating 50 mL of As(V) solution containing $Na_2HAsO_4 \cdot 7H_2O$ (10, 50, 100, 200 and 400 mg) with 10 mg adsorbent at pH, which was initially adjusted using 0.1 N, 1 N NaOH and HCl standard solution. After arsenate removal, all of the experimental procedure such as calculating E% was the same as the above adsorption experiment of heavy metal ions. To investigate the possibility of reusable adsorbent, desorption process were conducted with0.1 N NaOH (50 mL). The mixture of metal anions loaded adsorbents and solution to desorb was shaken for 2 h followed by constant temperature incubator shaker at 25℃. The adsorption efficiency experiments were carried out in triplicates with standard deviation of %. The value of isotherm parameters was determined by a fitting with Langmuir equation using ORIGIN program. The adsorption and recovery test toward Cr(VI) was performed with a stock solution, which was prepared with $K_2Cr_2O_7$ (10 mg) in distilled water (1 L), corresponding with adsorption experiments for As(V). The equilibrium adsorption tests for calculating the maximum capacities of Cr(VI) were accomplished with 50 mL of Cr(VI) solution containing $K_2Cr_2O_7$ (10, 50, 100, 200 and 400 mg) with 10 mg adsorbent at pH 4.5. All of the experimental procedures were carried out equal to adsorption and recovery test of As(V).

conditions	Adsorption	Desorption
pH	8.0±0.02	2.0±0.02
Time	2 h	2 h
Temperature	Room temperature	Room temperature
Rate of stirring	170 rpm	170 rpm

Table 1. Experimental conditions for adsorption and desorption of Cu(II) and Pb (II) by P-MG

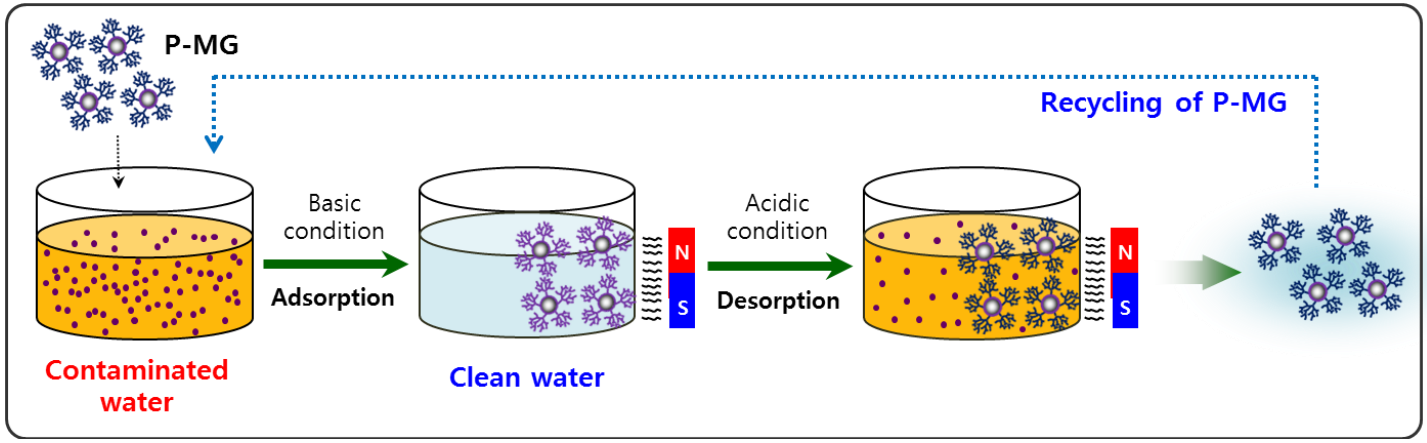

Figure 8. Illustration of adsorption and recovery system toward Cu(II) and Pb(II) by P-MG

conditions	Adsorption	Desorption
pH	4.5,6.0,8.0±0.1	12.0±0.5
Time	2 h	2 h
Temperature	Room temperature	Room temperature
Rate of stirring	200 rpm	200 rpm

Table 2. Experimental conditions for adsorption and desorption of As (V) and Cr(VI) by QP-MG

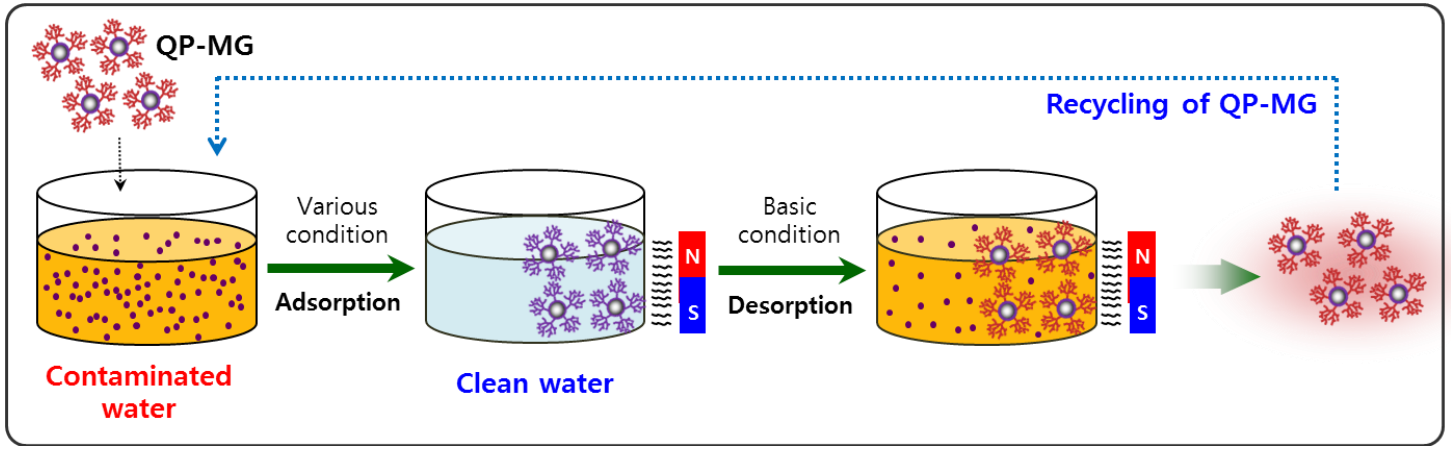

Figure 9. Illustration of adsorption and recovery system toward As(V) and Cr(VI) by QP-MG

3. Results and Discussion

3.1. Characteristics of b-PEI

3.1.1. FT-IR and ^{13}C NMR

We analyzed used b-PEI in studies to clarify its qualitative and quantitative characteristics. FT-IR spectrum of the used b-PEI is shown in Figure 10. There are specific peaks, which are related to amine-rich structure in a polymer chain. There are N-H stretching at 3300-3500 cm^{-1}, N-H bending (scissoring) at 1550-1650 cm^{-1} and -NH_2&N-H bending (wagging) vibrations at 660-990 cm^{-1} due to primary, secondary and tertiary amine groups in b-PEI. Its vibrations were presented at 3400, 1597 and 917 cm^{-1}. Peaks related to carbon in polymers were appeared at 2938 cm^{-1} of sp^3 C-H stretching, (1458 cm^{-1},1295 cm^{-1} and 1355 cm^{-1}) of CH_2&CH_3 bending, (1120 cm^{-1},1049 cm^{-1}) of C-N stretching vibrations. The sp^3 C-H stretching, CH_2&CH_3 deformation and C-N stretching vibrations are generally are shown up at 2850-3000 cm^{-1}, 1350-1470 cm^{-1} and 1000-1250 cm^{-1}. The results suggest that b-PEI is amine-rich polymer, which can be capable of chelating heavy metal ions from contaminated water.

The b-PEI was analyzed by ^{13}C NMR for understanding of branched structures. The ^{13}C NMR spectrum of b-PEI is shown in Figure 11. There are eight principal peaks, which is evidence of structural information. The peaks assignments for b-PEI, listed in Table 3. The most prominent feature of branched polymers is their degree of branching (DB) or branching factor, which defines the ratio of branched, terminal and linear units in the macromolecular structure [24]. The DB of this polymer can be defined as these data and followed equation:

$$DB=\frac{2D}{(2D+L)}$$

,where D and L represent the number of dendritic and linear units per macromolecule. The values obtained by inverse gated ^{13}C NMR spectroscopy correspond to DB of 0.38 and these results are summarized in Table 4. The DB of a perfect dendrimer equals 1, while a linear polymer has a DB of 0. The ratio of amine types in given by 1°: 2°: 3° = $(R_7+R_8+R_9)$: $(R_4+R_5+R_6)/2$: $(R_1+R_2+R_3)/3$. Our results give 1°: 2°: 3° = 2.11: 3.76: 1.13 or 30% 1°, 54% 2° and 16% 3°.

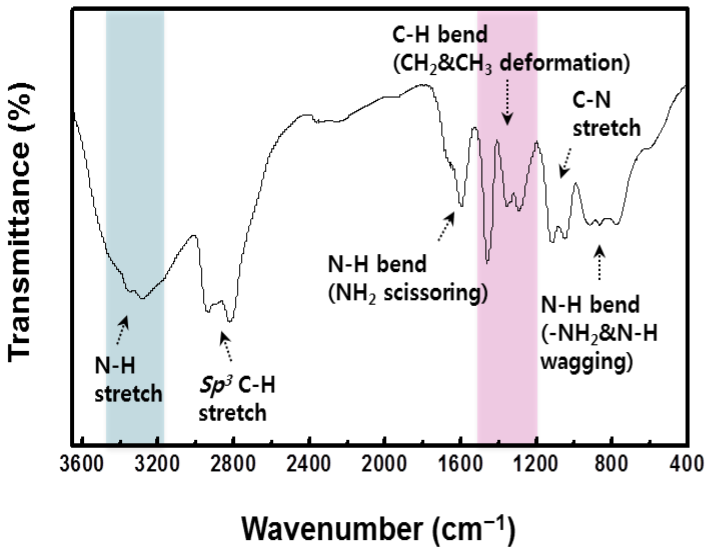

<Stretching vibrations>

- N-H stretching: 3300-3500 cm^{-1}
- Sp^3 C-H stretching: 2850-3000 cm^{-1}
- C-N stretching: 1000-1250 cm^{-1}

<Bending vibrations>

- N-H scissoring bending: 1550-1650 cm^{-1}
- CH_2&CH_3 deformation bending: 1350-1470 cm^{-1}
- NH_2&N-H wagging bending: 660-900 cm^{-1}

Figure 10. FT-IR spectrum of the b-PEI (branched, M_w=25,000)

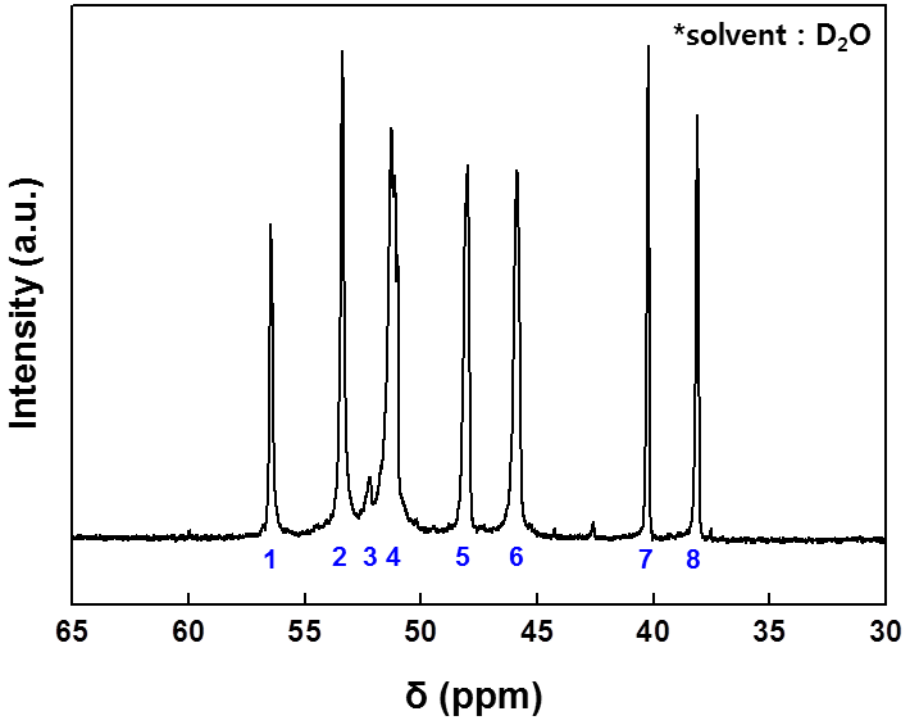

Figure 11. Inverse gated ^{13}C NMR spectrum of b-PEI

Region	Structure unit	δ (ppm)	Relative integral (R)
1	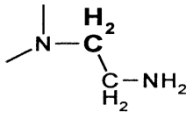	56.4	1.00
2	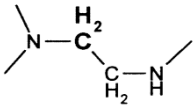	53.3	2.04
3	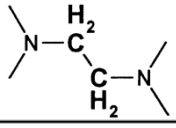	52.1	0.36
4	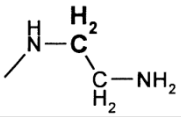	51.1	3.63
5	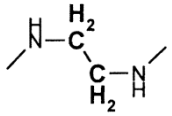	47.9	1.87
6	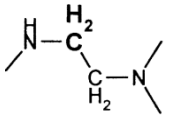	45.8	2.01
7	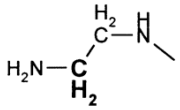	40.1	1.05
8	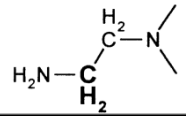	38.0	1.06

Table 3. Integral ratios of the ^{13}C NMR peaks of b-PEI

Amine group	Structural unit	Relative abundacnce (%)
1°	Terminal (T)	30
2°	Linear (L)	54
3°	Dendritic (D)	16

Table 4. DB of b-PEI (1°,2°,3° amine ratio)

3.2. Characteristics of P-MG and QP-MG

3.2.1. Crystal structure and morphology analysis

To introduce the various functional groups easily on the surfaces of the magnetite particle, AMG modified with amine functional groups was synthesized by facile one-pot hydrothermal process. The crystalline structure, crystallite size and phase purity were determined by WXRD. The diffraction peaks present in Figure 12a show that AMG has relatively strong and well-defined reflection peaks in the 2θ region of 20°–80°. The positions and relative intensities of all diffraction peaks corresponding to the (1 1 1), (2 2 0), (3 1 1), (2 2 2), (4 0 0), (4 2 2), (5 1 1), (4 4 0) and (5 3 3) plane were provided clear evidence for a cubic spinel structure, confirming the magnetite phase. (Joint Committee on Powder Diffraction Standards, JCPDS card, No. 19-0629).

After modification by b-PEI and GTA, the P-MG and QP-MG have relatively weak intensities. But, they have the same diffraction peaks with (1 1 1), (2 2 0), (3 1 1), (2 2 2), (4 0 0), (4 2 2), (5 1 1), (4 4 0) and (5 3 3) in Figure 12b. All of the diffraction peaks of the AMG, P-MG and QP-MG have no peaks characteristic of impure phases and were indicated well-crystallized magnetite phases. The WXRD results were used for the crystallite domain size determination of the AMG, P-MG and QP-MG based on the FWHM values for

the (2 2 0), (3 1 1), (4 0 0), (4 2 2), (5 1 1) and (4 4 0) reflections. The values of the main diffraction peaks and crystallite size for magnetite are listed in Table 5. The average crystallite size of the AMG, P-MG and QP-MG was estimated about 19.4 nm using *Debye–Scherrer* equation.

<Debye-Scherrer equation>

$$D = \frac{K\lambda}{\beta \cos\theta}$$

(K = 0.89, λ = Wavelength, 0.154 nm, β = Full width at half maximum,
θ = Bragg angle)

This result was consistent with the TEM images. AMG was well crystallized with inter-planar distance of *ca.* 0.25 nm, which was consistent with the lattice spacing of the (3 1 1) spinel planes of the crystal (see Figure 13c). And the AMG are formed sub-microspheres of about 200 nm by agglomerated magnetic nanoparticles. After modification, the P-MG and QP-MG were well crystallized with the lattice spacing of the (3 1 1) spinel planes of the crystal using Fast fourier transform (FTT) (Figure 14c, Figure 15d). All particles are formed sub-microspheres of about 200 nm due to the inter-particle

connections between agglomerated nanoparticles of about 18-22nm through the hydrothermal reaction systems. The sub-microspheres (100-400 nm) are effective separated from aqueous solution by applying an external magnetic field. Thus all the adsorbents are separated effectively from water treatment process by external magnetic field and could be regenerated to adsorb the toxic metal ions repeatedly.

AMG, P-MG and QP-MG were similar morphology, which was agglomerated to spheres. In case of the QP-MG, surface of the magnetite particles was covered with organic materials like polymers (see Figure 15a, b and c). Thick organic materials piled up surface of the QP-MG were inferred that P-MG was successfully modified with quaternary ammonium group by GTA.

Figure 16 shows the magnetic property of the adsorbents measured using a VSM with applied field from –10 to +10 kOe. The magnetization curve showed reversible characteristics with no hysteresis. This property was indicated that the magnetic adsorbents of the P-MG and QP-MG have paramagnetic behavior and feasible to reversible separation at external magnetic field. The saturation magnetization value, M_s for AMG, P-MG and QP-MG at 10 kOe was 82.3 emu/g, 67.4 emu/g and 63.7 emu/g, which could be enough for the repeated magnetic separation. The M_s of 60-80 emu/g were expected

value for efficient separation and recovery of the adsorbents from water [20]. When possessing in a vial, adsorbents were attracted by a conventional magnet placed close to the vial wall, and could be re-dispersed within a few minutes when the magnet was removed.

These results suggest that adsorbents were retained constantly high magnetization after surface modifications by b-PEI and GTA and possible to apply for water treatment process efficiently. The FE-SEM was also employed to visualize the morphology and bulk structure of the AMG, P-MG and QP-MG (see Figure 17, 18 and 19). Figure 19 shows FE-SEM images of the QP-MG, from which sub-microspheres with diameter in the range of 100-200 nm were observed. Figure 17 and Figure 18 show the image of the AMG and P-MG which have spherical morphologies and rough surfaces. And all clusters have pores or holes due to the agglomerated nanoparticles. These results were indicated that modification of the P-MG and QP-MG did not affect significantly their morphologies and structures.

The combined results of WXRD, TEM, SEM, and VSM were revealed that AMG, P-MG and QP-MG were retained constantly magnetite phase, morphology, and magnetization after surface modifications by b-PEI and GTA. Thus, these adsorbents could be possible to use as efficient adsorbents.

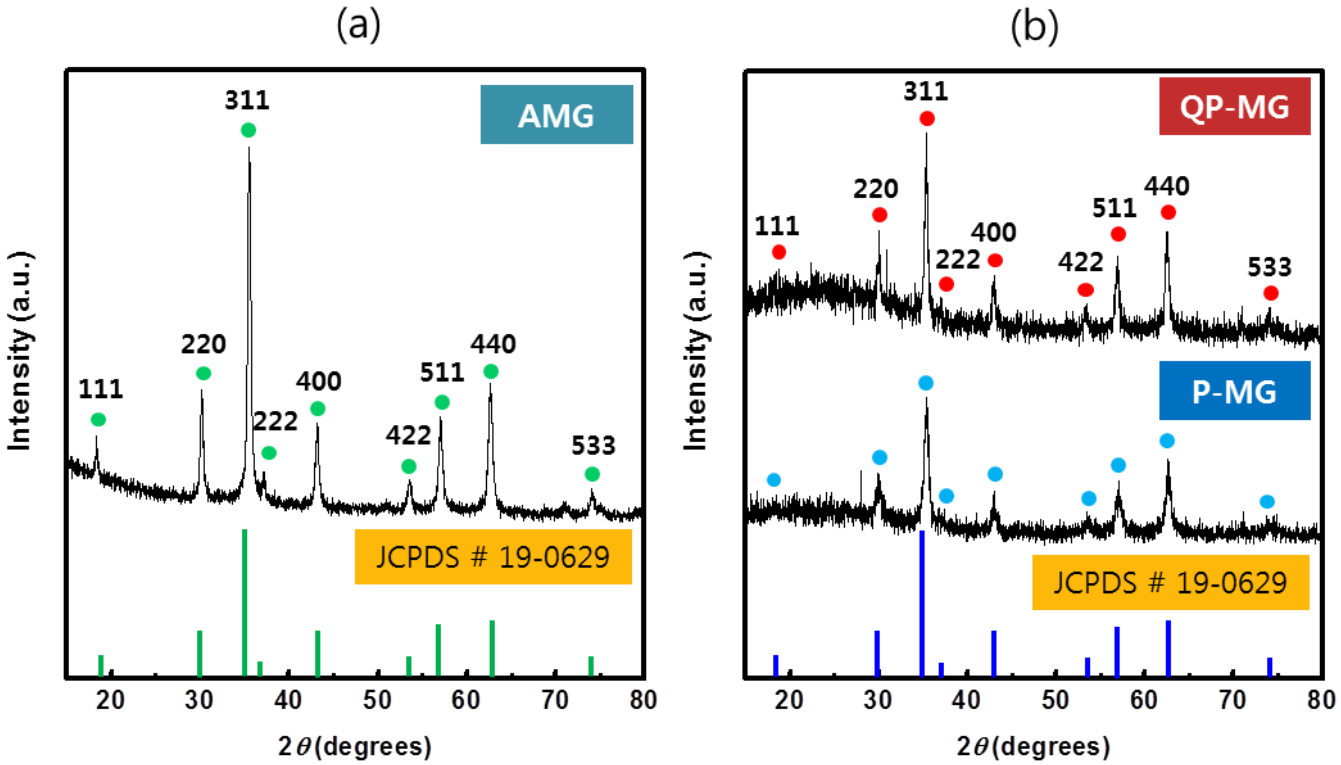

Figure 12. WXRD spectra of synthesized AMG, P-MG and QP-MG

h k l	2θ (deg.)	*d*-spacing (nm)	Intensity (a.u.)	FWHM (2θ)	Crystallite size (nm)
2 2 0	30.02	0.30	49.0	0.44	18.49
3 1 1	35.36	0.25	100.0	0.42	19.64
4 0 0	43.00	0.21	36.1	0.38	22.23
5 1 1	56.92	0.16	43.7	0.46	19.43
4 4 0	62.48	0.16	56.4	0.50	18.38
7 3 0	89.84	0.11	25.2	0.60	18.50

Table 5. FWHM values of the main diffraction peaks and crystallite size for magnetite

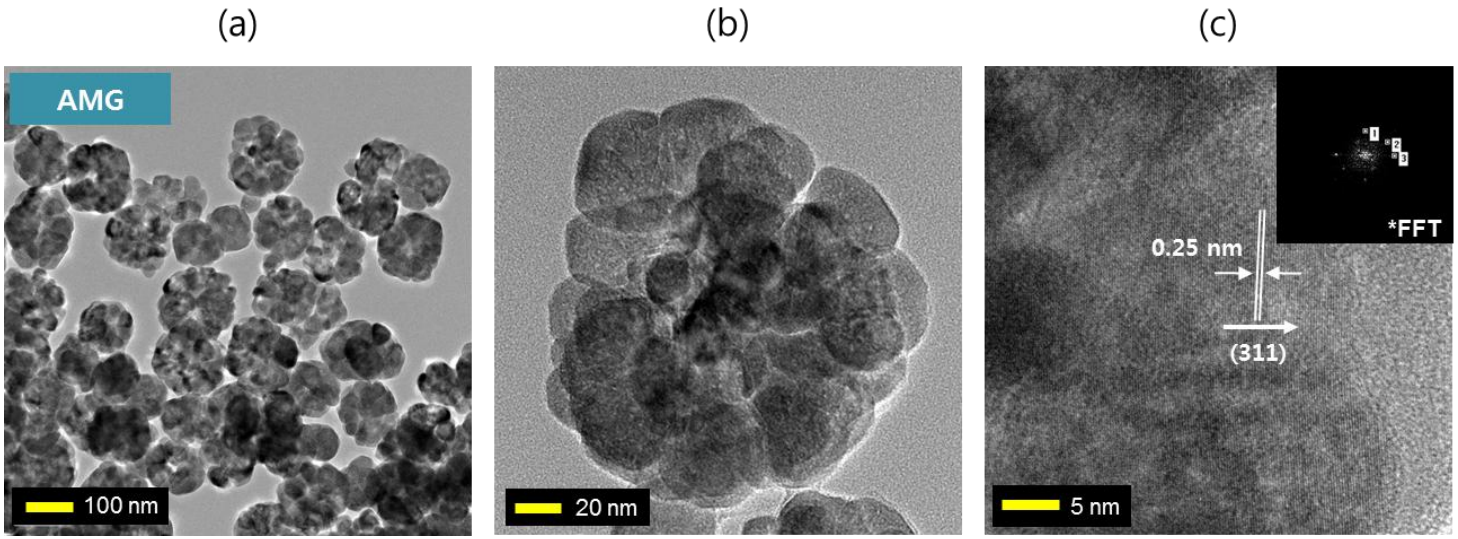

Figure 13. HR-TEM images of AMG; (a) spherical morphology of particles (b) A magnified particle (c) Lattice spacing of the spinel planes of the crystal

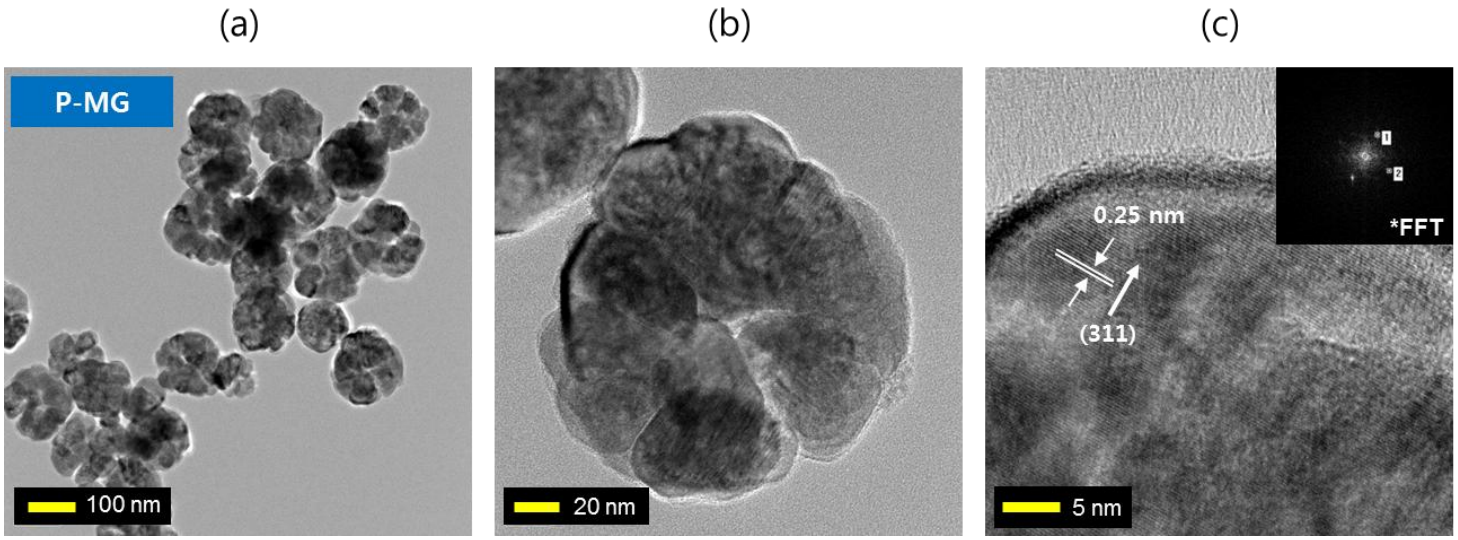

Figure 14. HR-TEM images of P-MG; (a) spherical morphology of particles (b) A magnified particle (c) Lattice spacing of the spinel planes of the crystal

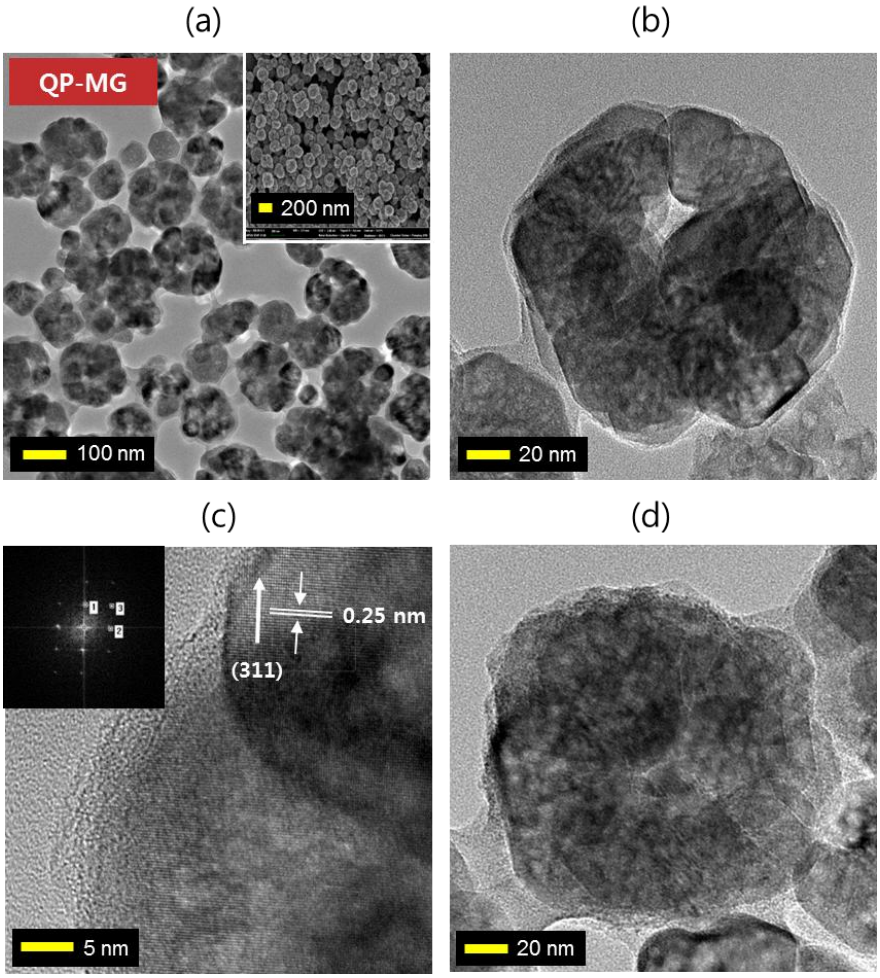

Figure 15. HR-TEM images of QP-MG; (a) spherical morphology of particles (b) A magnified particle(c) Lattice spacing of the spinel planes of the crystal (d) Piled-up surface with polymer of particles

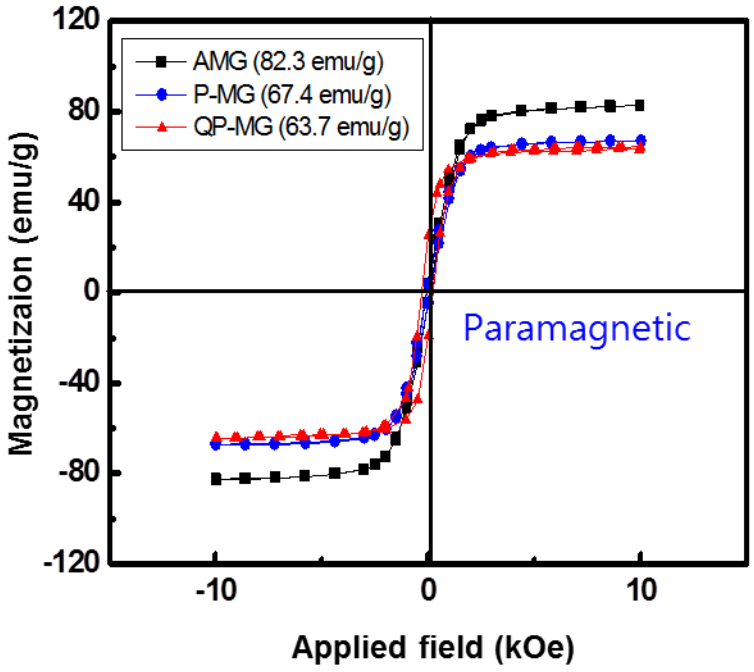

Figure 16. Magnetization curve of AMG, P-MG and QP-MG

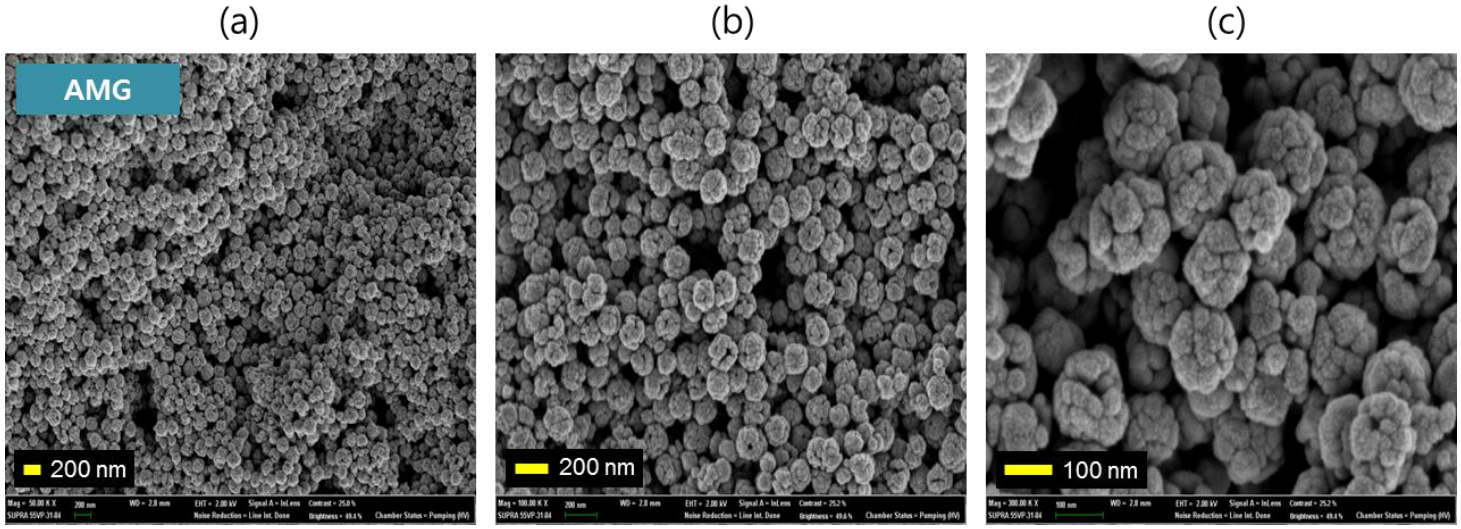

Figure 17. FE-SEM images of AMG

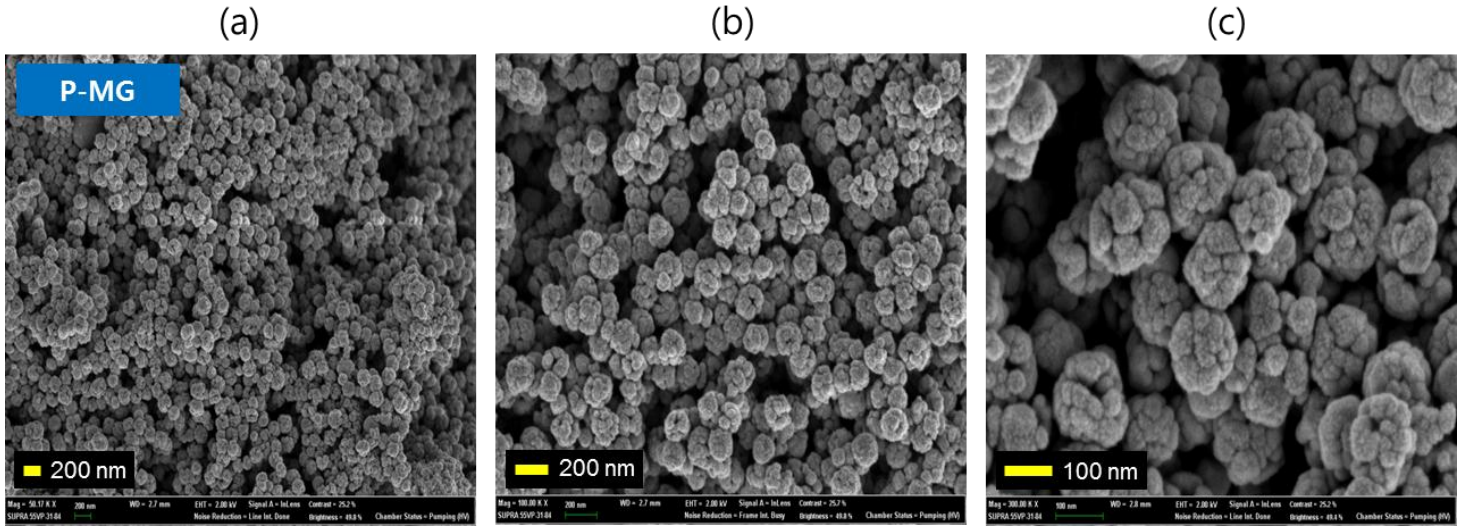

Figure 18. FE-SEM images of P-MG

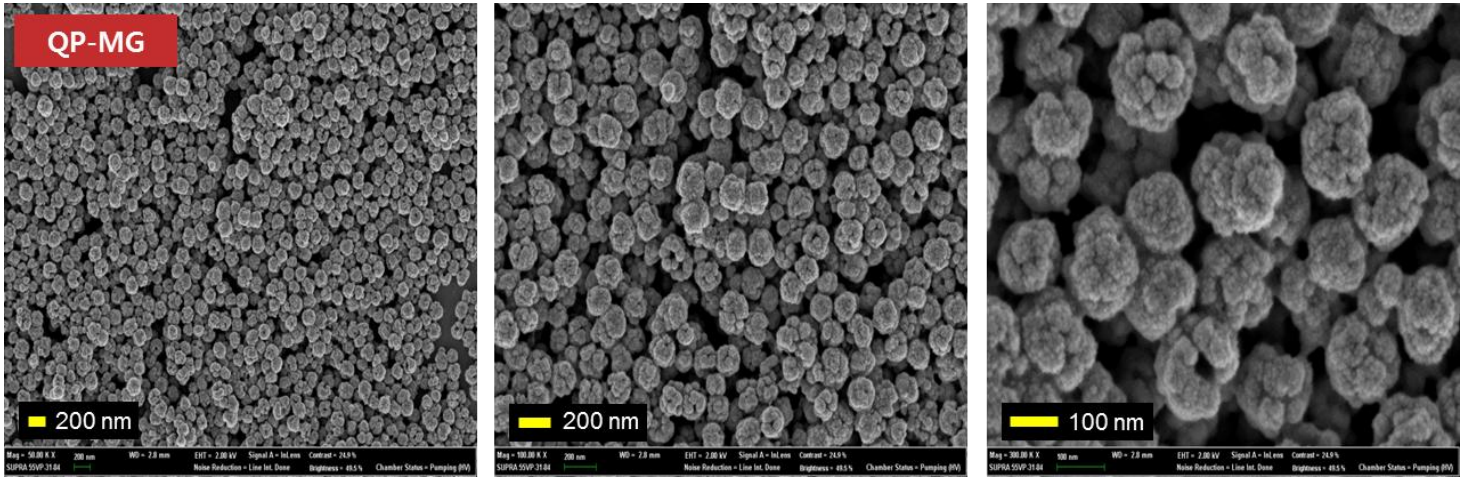

Figure 19. FE-SEM images of QP-MG

3.2.2. FT-IR and EA

The FT-IR spectra of the AMG contained peaks that corresponded to following functional groups : N-H stretching (3424 cm^{-1}), sp^3 C-H stretching (2927 cm^{-1}), N-H vibration (1640 cm^{-1}), C-H bending (1406 cm^{-1}), C-N stretching (1055 cm^{-1}), Fe-O vibration (576 cm^{-1}). The observed band at 3424 cm^{-1}, 1640 cm^{-1} and 2927 cm^{-1} were associated with $–NH_2$ stretching, N–H bending vibrations of the amine groups, and sp^3 C–H stretching of the alkyl chain, respectively. These were indicated that amine group was immobilized on the magnetite particles by 1,6-hexadiamine.Other absorption bands at 1406 cm^{-1}, 1055 cm^{-1} and 576 cm^{-1} were corresponded to C-H bending, C-N stretching and Fe-O bond vibrations of iron at tetrahedral sites.

Figure 20a shows the FT-IR spectrum of the P-MG, containing the same peaks with the AMG. After assembly of the b-PEI to the AMG, the intensity of N-H stretching (3424 cm^{-1}) band was increased in P-MG. The elemental analysis (EA) data of the P-MG is listed in Table 6. The nitrogen content and the atomic ratio of carbon/nitrogen (C/N) in the P-MG were measured by EA. The carbon and nitrogen contents are 1.87 wt% and 0.952 wt%. The carbon to nitrogen ratio of the P-MG was about 1.97 and similar to 2.00. Chemical structure the b-PEI considered in Figure 21, the C/N ratio of b-

PEI is 2.00. The result reflects that b-PEI was introduced the surface of magnetite indirectly. The combined results of FT-IR and EA were revealed that the magnetite surface was successfully modified by cyanuric chloride and b-PEI in the process.

In comparison with AMG and P-MG, a new CH_3-N^+ stretching peak (Figure 20b), at around 1470-1480cm^{-1} for QP-MG was appeared, probably due to the quaternary ammonium groups [25,26]. In addition, it was observed that the characteristic peaks of N-H stretching, N-H vibration and C-N stretching were unchanged in QP-MG compared to AMG and P-MG. Therefore, it can be implied that quaternary ammonium group was successfully conjugated to the amine groups of the P-MG through the quaternization.

The combined results of FT-IR and EA were indicated the successful modification in the adsorbents. Transition of the specific peaks (N-H stretching and CH_3-N^+ stretching) and nitrogen contents in P-MG and QP-MG was demonstrated that amine group and quaternary ammonium group were introduced to magnetite by b-PEI and GTA.

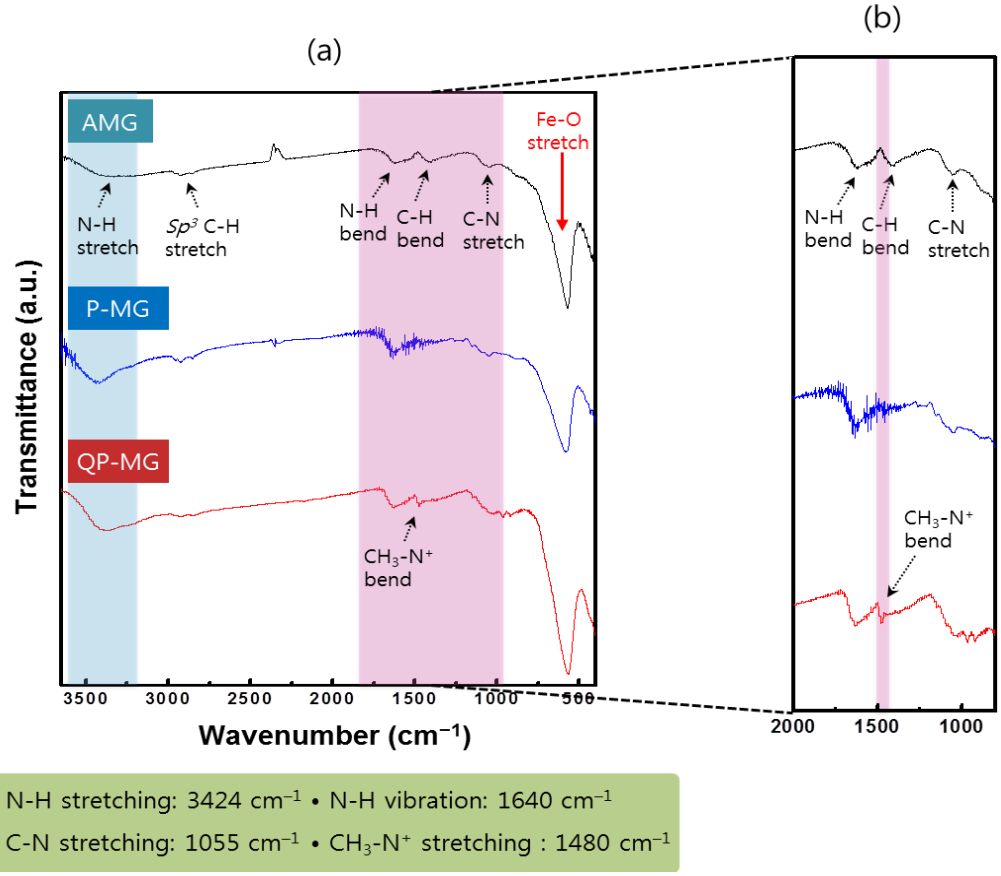

Figure 20. FT-IR spectrum of synthesized magnetic particles; (a) FT-IR spectrum of AMG, P-MG and PQ-MG (b) CH_3-N^+ peak of QP-MG

Element / Sample	Nitrogen (wt%)	Carbon (wt%)	C/N ratio
P-MG	0.952	1.87	1.97

Table 6. EA data of P-MG

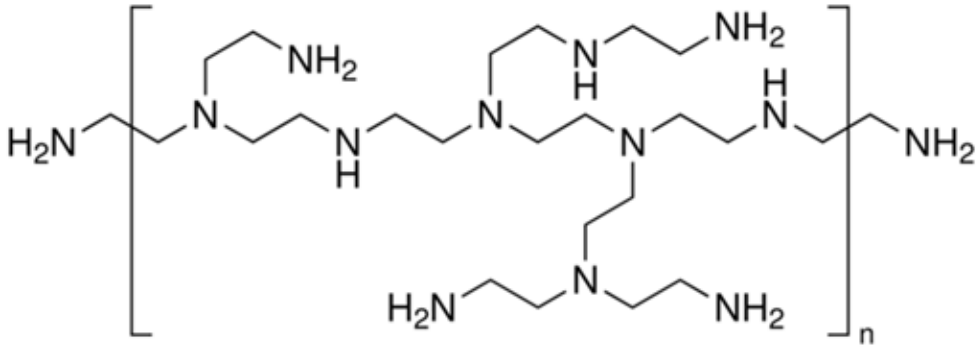

Figure 21. Chemical structure of b-PEI

3.2.3. XPS and TGA

More specific information about the composite clusters was obtained using XPS. The XPS was conducted to identify the chemical states and the quantitative analysis of atoms in the adsorbents. Figure 22 shows XPS analysis of the AMG, P-MG and QP-MG. The Fe *2p* spectrum in Figure 22a shows peaks at 710 and 724 eV, corresponding to binding energy of $2p_{2/3}$ and $2p_{1/2}$ spin-orbital components of magnetite. The Fe signal of the AMG, P-MG and QP-MG appeared at equal positions was manifested that the adsorbents remained iron oxide structure.

N l*s* XPS signals involve different types of nitrogen bonding configurations: pyrrole-like (399-401.2 eV), quaternary (401.1-402.7 eV). The most relevant C-N XPS bonding peaks are found at 398.7-400.5 eV for amine (>N- and –NH-). The primary, secondary, tertiary amine functional group are confirmed in the N1*s* spectrum (see Figure 22b), where the binding energy peaks at 399.7 eV, 398.7 eV, 398.9 eV are attributed to the formation of an amine on the surface of the AMG, P-MG and QP-MG.

The most relevant C-N XPS bonding peaks were found at 284-288 eV for carbon. In the P-MG case, the major carbon peak was near 285 eV and is consistent with carbon in a nitrogen-rich environment (see Figure 22c).

Intensities of the characteristic peaks of the carbon and nitrogen were increased in the modification process by b-PEI.

Through the XPS quantitative analysis, mass concentration of the nitrogen in the AMG and P-MG were measured 0.84±0.10% and 4.46±2.84%. In the P-MG, the mass concentrations of nitrogen were higher than that of the AMG by the modification process. Calculated from the quantitative XPS data, mass concentration of the nitrogen in the P-MG was *ca.*3.61%. Changes in the peak areas were provided useful information about the surface loading of the amine and b-PEI onto magnetite.

In the QP-MG case, the N 1*s*signalobserved at higher binding energy ($C\text{-}N^{+}$, 401.1-402.7 eV) than N 1*s* peak of P-MG is attributed to quaternary ammonium polyethylenimine (see Figure 22b). The N 1*s* peak shifting of QP-MG was due to the electron-withdrawing power of the nitrogen group in quaternary ammonium. After quaternization, intensity of the characteristic peak and nitrogen contents were increased in comparison with AMG and P-MG. The contents of nitrogen in the QP-MG were measured about 7.31% using XPS quantitative analysis (see Table 7) and mass concentration of the nitrogen in the its calculated from this data was *ca.* 2.84%.

This result was consistent with the TGA. The TGA was employed to quantify the loading of b-PEI and quaternary ammonium polyethylenimine. As

shown in Figure 23, the major weight loss occurred between 100 ℃ and 500 ℃, indicating the decomposition of b-PEI and quaternary ammonium polyethylenimine (The water start to decompose at 0 ℃ and finish at 100 ℃). The weight losses of the organic component in AMG, P-MG and QP-MG were 3.49, 7.36 and 10.4 wt%. Calculated from the TGA data, the weight losses of the organic component in P-MG and QP-MG were *ca.* 3.87 and 3.04 wt%. Thus the P-MG was modified with about 3.87 wt% of b-PEI and the QP-MG was quaternization by about 3.04 wt% of GTA.

The combined results of XPS and TGA were demonstrated that the adsorbents were successfully modified with amine and quaternary ammonium group by b-PEI and GTA. The introduced amounts of the b-PEI and quaternary ammonium groups on magnetite surfaces were confirmed qualitatively and quantitatively.

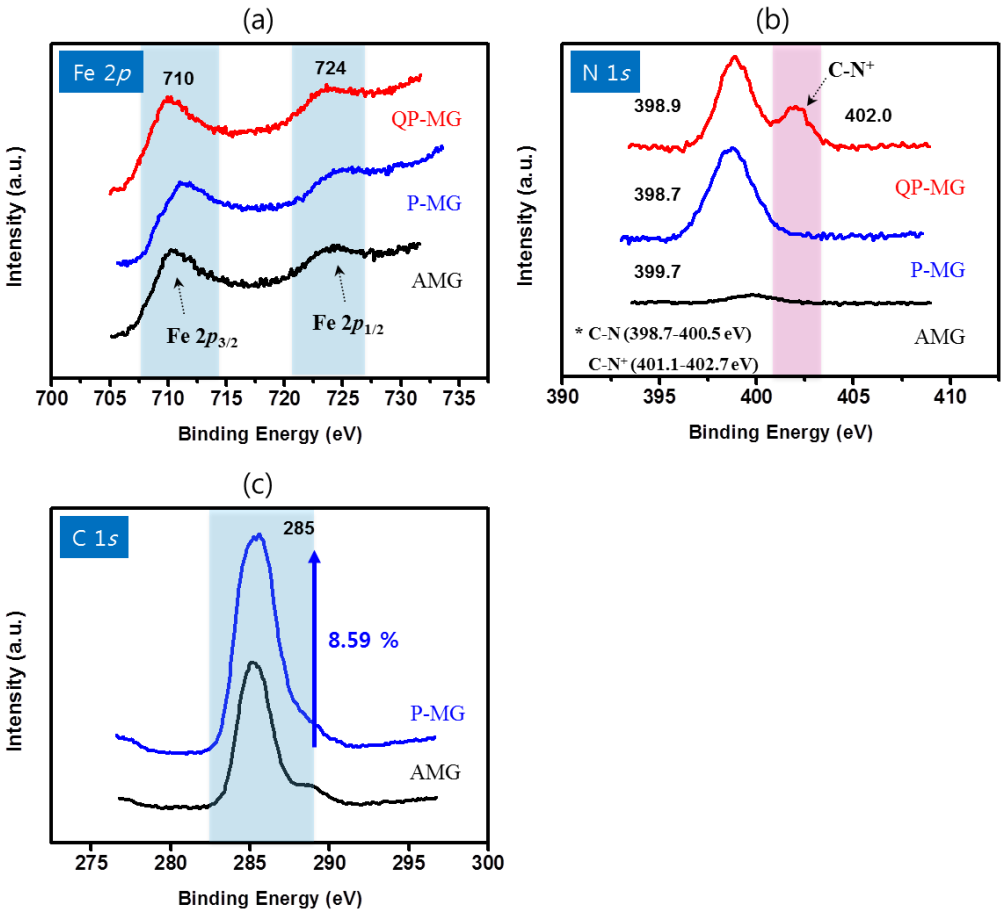

Figure 22. XPS spectrum of AMG, P-MG and QP-MG; (a) Fe 2*p* binding energy (b) N 1*s* binding energy (c) C 1*s* binding energy

XPS quantitative analysis			
Sample / Element	AMG	P-MG	QP-MG
Nitrogen (mass con.)	**0.84**±0.10	**4.46**±2.84	**7.31**±0.10

Table 7. XPS quatitative analysis data of AMG, P-MG and QP-MG

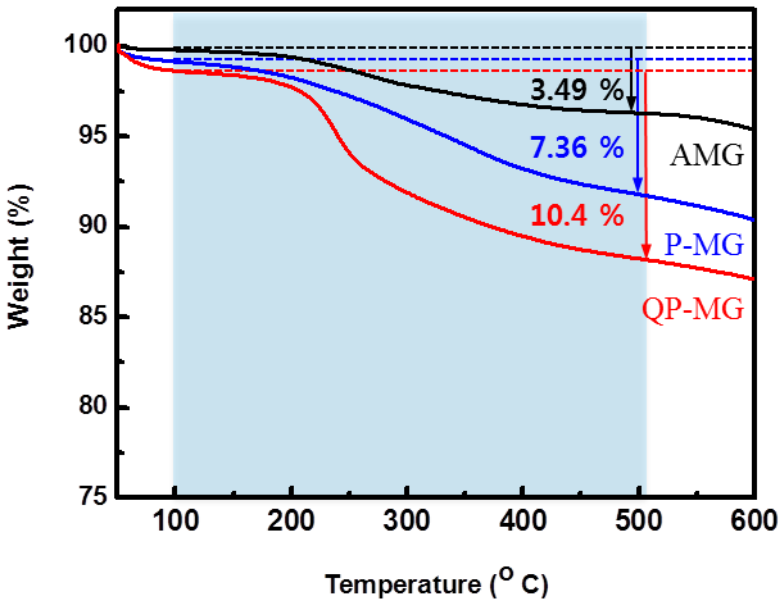

Figure 23. TGA results of AMG, P-MG and QP-MG

3.3. Evaluation of adsorption and recovery property of P-MG toward Cu(II) and Pb(II)

3.3.1. Adsorption property

A number of scientists were already studied to optimize for the adsorption conditions to remove heavy metal ions efficiently. The surface charge and the protonation degree of adsorbent are significantly influenced by the pH value. To know the pH for the most effective removal of heavy metal ions, adsorption test was carried out in different pH value (at 7.0, 8.0 and 9.0).

Most of metal ions are discharged at low level (~ppm) from industrial wastewater. In order to remove the toxic metals efficiently from contaminated water, adsorbents with high maximum capacities as well as applying at contaminated water including low concentration of heavy metal ions are very important. Thus, we were carried out adsorption tests for calculating adsorption efficiency in contaminated water including low level of the metal ions.

The adsorption experiments are described virtually in Figure 24. Before adsorption, contaminated water was prepared in vial (copper solution look like blue when its concentration is saturated). Black magnetic particles (adsorbents) were added to contaminated solution and stirred dispersedly for 2 h. After adsorption, the adsorbents were separated within a few minutes by

magnet. It could be re-dispersed within a few minutes when the magnet was removed.

Generally, degree of the protonation of b-PEI is decreased at basic conditions relatively. As high pH value, large amounts of OH^- might compete with H^+ for protonation, resulting in the decrease of degree of the protonation in b-PEI.

Adsorption mechanism to remove the heavy metal ions is known to chelating interaction between metal ions and adsorbents (see Figure 2). The surface of the adsorbents is deprotonated at basic conditions and chelating interaction between heavy metal and adsorbents works effectively at the conditions. Because of electrical repulsion force between the positive charged heavy metal ions and adsorbents became weaker in basic conditions. At high pH, the weak electrical repulsion force between adsorbent and cationic metal ions derive to chelate with the cationic metal ions, which is more feasible to access at adsorption site of b-PEI. With the increase of solution pH, electrical repulsion force and competition with H^+ became weaker, thus the adsorption of metal ions could be increased.

Thus adsorption test of the heavy metal ions were carried out at neutral and basic conditions. Figure 25 shows the adsorption efficiency of Cu(II) by the P-MG at various pH value. The adsorption efficiency (%), A% was calculated

as follow:

$$\mathrm{A}\% = \frac{(C_i - C_e)}{C_{\mathrm{i}}} \times 100$$

All of the adsorption efficiencies at pH 7.0, 8.0 and 9.0 were more than 86%. The maximum adsorption efficiency of Cu(II) was observed about 96.3% at pH 8 (see Figure 25). Taking into account the formation of metal hydroxide precipitation under high pH solution, the result that pH at 8.0 was feasible for effective adsorption of Cu(II) can be applied for removal conditions toward positive metal ions (two-electron positive ions). The adsorption efficiency of 97.2% achieved by P-MG toward Pb(II) at pH 8.0 is presented in Figure 26. The experimental data of adsorption efficiency toward Cu(II) and Pb(II) were reported as the average of triple determinations, and the standard deviations are around ±2.0. It was found that at fixed pH value, the adsorption efficiency for the two heavy metal ions was Pb(II) >Cu(II), implying the stronger affinity of the adsorbent for Pb(II) than Cu(II).

The response sensitivity of heavy metal ions and surface charge of the adsorbent in various pH affect for adsorption efficiency of the heavy metal ions.

Figure 24. Adsorption experimental pictures

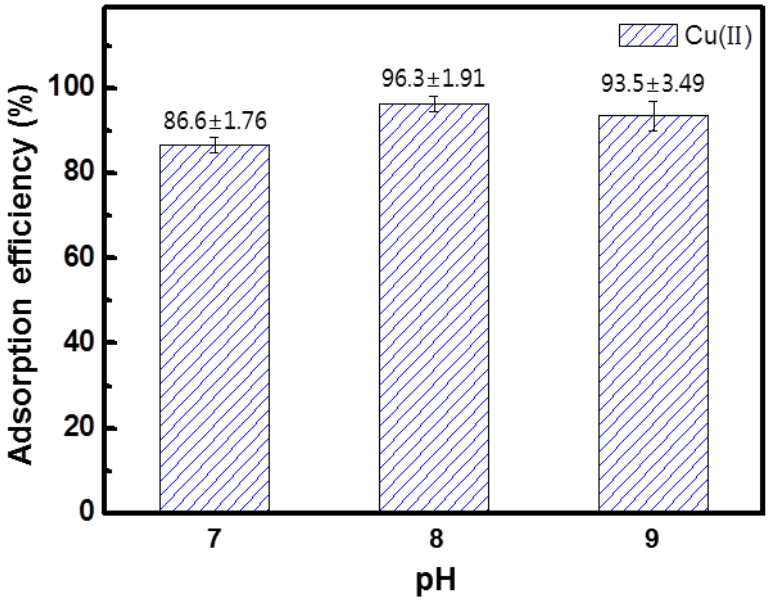

Figure 25. Adsorption efficiency of P-MG toward Cu(II) at various pH

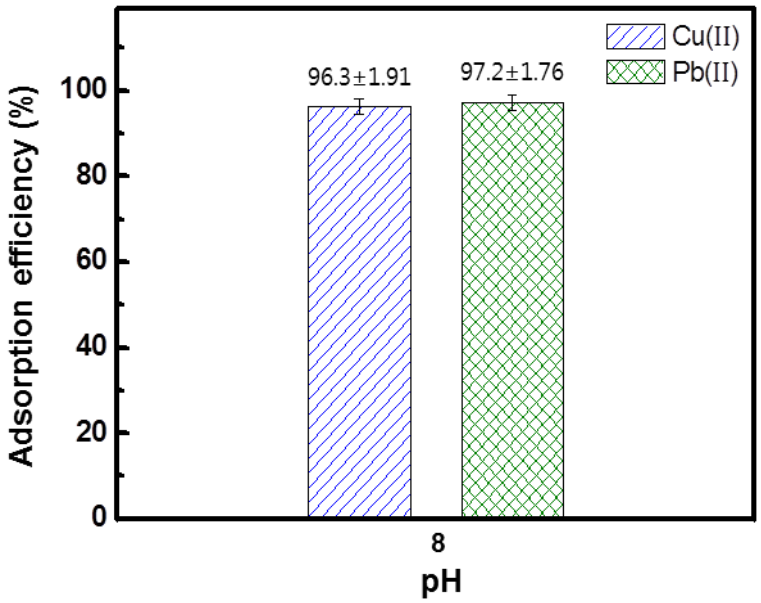

Figure 26. Maximum adsorption efficiency of P-MG toward Cu(II) and Pb(II) at pH 8.0

3.3.2. Equilibrium isotherm

Equilibrium isotherm governing the maximum adsorption capacity is one of the important characteristics that define the efficiency of adsorption. The equilibrium characteristics of adsorption have been used to describe with various isotherm equations including Langmuir, Freundlich, Redlich-Peterson, Langmuir-Freundlich, Toth, and Tempkin equations. Among these isotherm equations, Langmuir and Freundlich isotherms are commonly used in assumption of adsorptionperformance.

The Langmuir adsorption model based on the assumptions that the adsorption occurs in monolayer and all site are equal, is often applicable for modeling the adsorption on homogeneous surface sites. And there is no interaction among adsorbed ions. Its model is

$$q_e = \frac{q_m b C_e}{(1 + bC_e)}$$

$$\frac{1}{q_e} = \frac{1}{bq_m} C_e + \frac{1}{q_m}$$

,Where q_e (mg/g) is the amount of heavy metals adsorbed at equilibrium, C_e (mg/L) is the equilibrium metal concentration, b (L/mg) is the

equilibrium constant related to adsorption energy and q_m (mg/g) the maximum adsorption capacity [18].

The maximum adsorption capacity of the as-obtained P-MG for heavy metal ions was investigated at pH 8.0. The result for adsorption isotherms of Cu(II) and Pb(II) with corresponding Langmuir plot are presented in Figure 27 inset. The fitted constants along with regression coefficients R^2 are summarized in Table 8. The data was fitted well to the model with R^2 of 0.9932 and 0.9995.

Therefore, the adsorption of heavy metal ions onto P-MG occurs in monolayer and surface of the adsorbents is homogeneous. As listed in Table 8, the calculated maximum adsorption capacities of Cu(II) and Pb(II) were 158.7 mg/g and 163.9 mg/g. The q_m of P-MG toward Cu(II) and Pb(II) are similar or a bit high as compared with many reported results, as shown in Table 9.

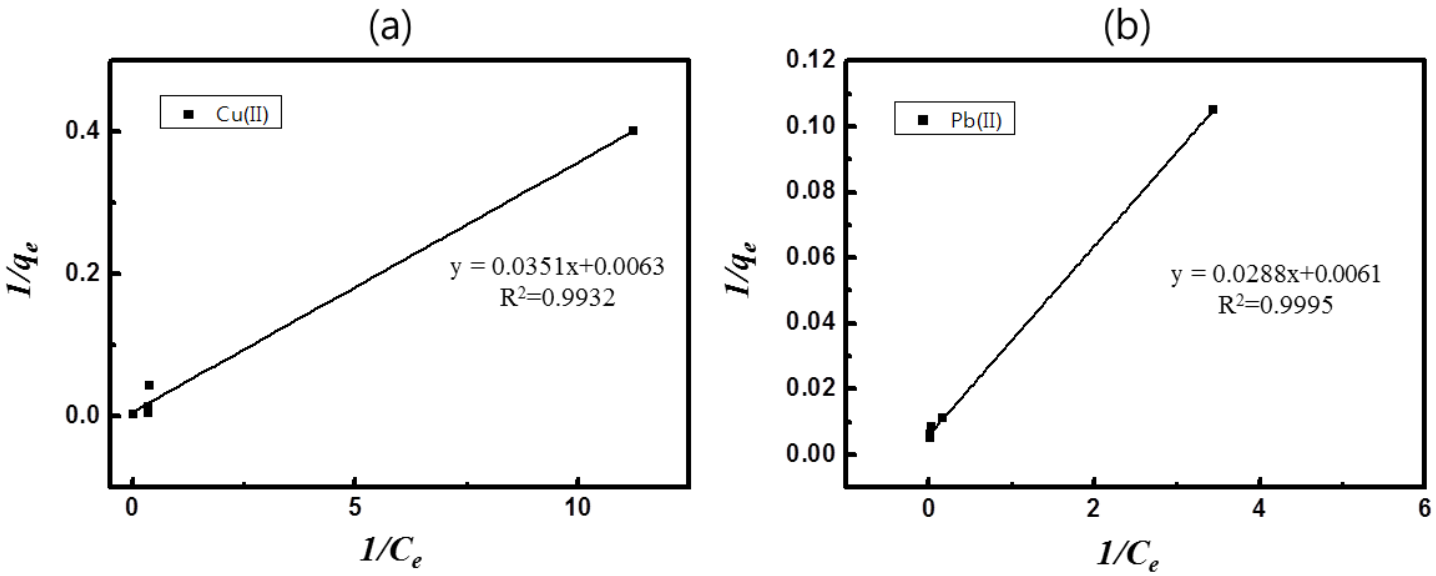

Figure 27. Equilibrium isotherms by Langmuir adsorption model; (a) Langmuir curve of Cu(II) (b) Langmuir curve of Pb(II)

Langmuir constant	Cu(II)	Pb(II)
q_m	158.7	163.9
b	0.4958	0.7305
R^2	0.9932	0.9995

Table 8. Langmuir constant and maximum adsorption capacity for Cu(II) and Pb(II)

References	Materials	Cu(II)	Pb(II)
Present study	**P-MG**	**158.7 mg/g**	**163.9 mg/g**
Ya pang *et. al* *Desalination* **2011**, *281*, 278-284	PEI-grafted magnetic porous powder	157.8 mg/g	n/a
Mahnaz mahdavi *et. al* *J. Inorg. Organomet. Polym.* **2013**, *23*, 599	SiO_2/(3-Aminopropyl) triethoxysilane-Coated Magnetite Nanoparticles	n/a	17.65 mg/g
Karl mandel *et. al* *Appl. Mater. Interfaces* **2012**, *4*, 5633	Modified Superparamagnetic Nanocomposite Microparticles	30 mg/g	n/a
Denizli *et. al* *Chem. Eng. J.* **2011**, *166*, 1144	magnetic beads containing triazole	151.5 mg/g	193.8 mg/g
Yuan *et. al* *J. Appl. Polym. Sci.* **2009**, *114*, 2246	mesoporous titania-silica-phosphonate hybrid material	46.3 mg/g	92.4 mg/g

Table 9. Maximum adsorption capacity of prepared P-MG and comparison materials toward Cu(II) and Pb(II)

3.3.3. Recovery property

To reduce the quantity of spent adsorbents and secondary contaminant in our environment, regeneration and recovery of used adsorbents, respectively, are very important. As it has been seen that the adsorption of Cu(II) and Pb(II) ions in P-MG was highly pH dependent; therefore we assumed that desorption of these ions may be possible in acidic conditions, because of repulsion between the cationic metal ions and protonated amine group in b-PEI.

In the present work, desorption studies were conducted using1 N HCl solution. The mechanism of desorption is that electrical repulsions between protonated amine group of b-PEI and heavy metal ions (two-electron positive ions) at acidic conditions (see Figure 2). The recovery experiments were carried out to repeat the 4 cycles by regenerated adsorbents. (One cycle includes adsorption and desorption processes by already used adsorbents.)

The recovery efficiency, R% was determined following equation:

$$\text{R \%} = \frac{Q_r}{Q_i} \times 100$$

,where Q_i is the uptake of heavy metal ions and Q_r is the uptake of

heavy metal ions after the regeneration procedure. The R% and A% of the P-MG toward Cu(II) and Pb(II) show in Figure 28. After 4 recycle tests, the A% and R% of recycled the adsorbents were more than 90% and 94% toward cationic heavy metals.

It was attributed that structural advantages of the b-PEI can be feasible for adsorption and desorption of the heavy metal ions. The results suggest that the P-MG has high recovery efficiency and adsorption efficiency could show great application prospects in contaminated water treatment.

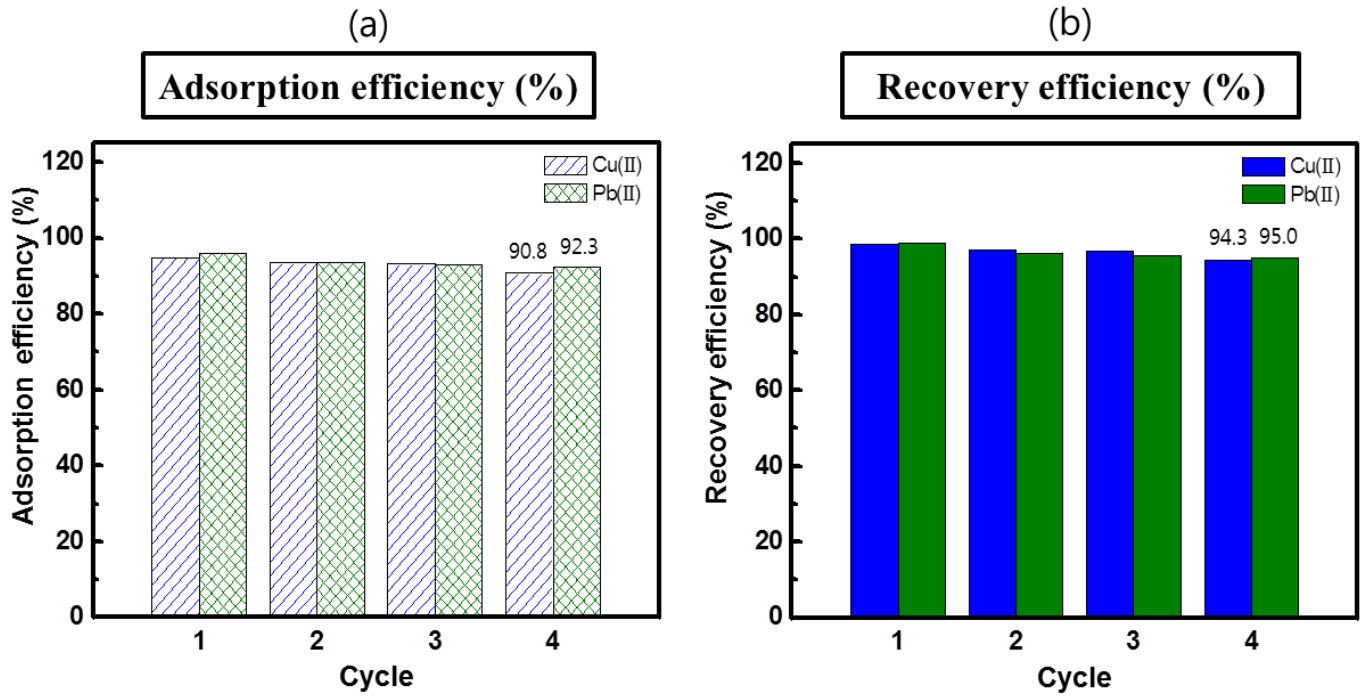

Figure 28. Adsorption and recovery efficiency of P-MG toward Cu(II) and Pb(II), after 4 recycle test

3.4. Evaluation of adsorption and recovery property of QP-MG toward As(V) and Cr(VI)

3.4.1. Optimization of QP-MG

In order to remove the arsenate from contaminated water, the optimization and preparation of the QP-MG could be very much desirable. Quaternization for surface modifications of cellulose, chitosan and polymer have been studied, which is used as binder for negative charged protein in genes delivery application. In coherence, the amine groups in b-PEI have positive charge by quaternization, it could combine with anionic metals form water.

In present work, the synthesis of quaternary ammonium functionalized b-PEI was carried out using a modified process with glycidyltrimethylammonium chloride (GTA) described previously.

We supposed that adsorption capacities are affected in degree of positive charge with quaternary ammonium functional group. Therefore adsorption experiments were carried out as volume of GTA for optimizing the scheme to prepare the QP-MG. Adsorption efficiencies of As(V) at pH 8.0 were increased by elevating volumes of GTA (see Figure 29). Degree of quaternization was significantly influenced by volumes of the GTA. Maximum removal efficiency of As(V) was observed about 87.6% at pH 8.0 by QP-MG

synthesized with GTA 25 mL. Thus, QP-MG was optimized with GTA for efficient removal of the arsenate and it could be applied to adsorption experiments.

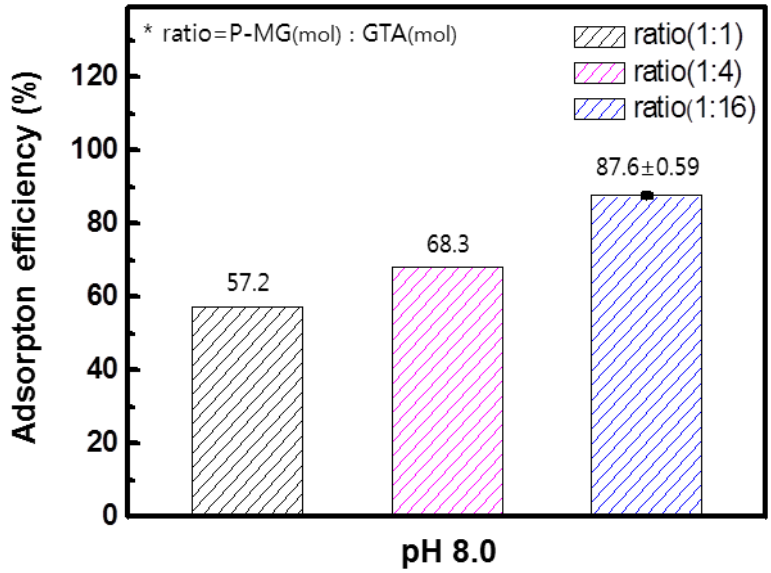

Figure 29. Adsorption efficiency of prepared QP-MG as ratio of GTA toward As(V)

3.4.2. Effect of pH on adsorption property toward As(V)

Studies to remove the arsenics have been investigated in acidic or basic conditions by many researchers. The adsorption of arsenate is highly dependent with pH; Because arsenate (As(V)) exists various formation such as H_3AsO_4, $H_2AsO_4^-$, $HAsO_4^{2-}$, AsO_4^{3-} in pH conditions (see Figure 30). We suppose that this characteristics effect adsorption and recovery efficiency. Thus adsorption experiments to evaluate the removal efficiency were carried out in various pH values at 4.5, 6.0 and 8.0. Reason for choosing this is the fact that amounts of one-electron negative ion ($H_2AsO_4^-$) and two-electron negative ion ($HAsO_4^{2-}$), respectively, are the highest at pH 4.5 and 8.0 in various pH conditions.

Adsorption efficiencies of the As(V) are show in Figure 31 and were increased as increasing of the pH value. The adsorption efficiency was calculated with mentioned equation in section 3.3.1. The A% of 71.9%, 82.4% and 87.6% were achieved at pH 4.5, 6.0 and 8.0. The experimental data of A% toward As(V) was reported as the average of triple determinations, and the standard deviations are around ±0.7

The highest and the lowest A% were presented at the pH 8.0 and 4.5, respectively, among the pH conditions. The A% was affected by discrepancy of interaction between QP-MG and As(V).

The mechanisms of the adsorption with arsenate on QP-MG are described in Figure 3. Positive charged the functional groups (quaternary ammonium) on the adsorbents form surface may complex with the arsenate via electrostatic attraction and ionic bond interaction. The positively charged R_3N^+ at the surface of adsorbent could attract negatively charged $H_2AsO_4^-$ and $HAsO_4^{2-}$ by electrostatic attraction.

Most of the arsenate anions at pH 8.0 and pH 4.5 exists two-electron negative ions ($HAsO_4^{2-}$) and one-electron negative ions ($H_2AsO_4^-$). At pH 8.0, interactions of the adsorbent with $HAsO_4^{2-}$ may be stronger than that of at pH 4.5. Thus, the strong interaction between adsorbent and $HAsO_4^{2-}$ such as an ionic bond leads to the high removal efficiency at pH 8.0. We supposed that intensities of the ionic bond interaction are alternated by changing the pH conditions and affect to regeneration efficiency toward As(V). Regeneration studies with various pH conditions are managed to confirm our supposition in next section 3.4.3.

The results suggest that A% is affected to discrepancy of interaction between the adsorbents and As(V) in various pH conditions. Thus, the maximum adsorption efficiency of QP-MG toward As(V) was 87% at pH 8.0. It might be induced strong interactions with As(V) than that of pH 4.5.

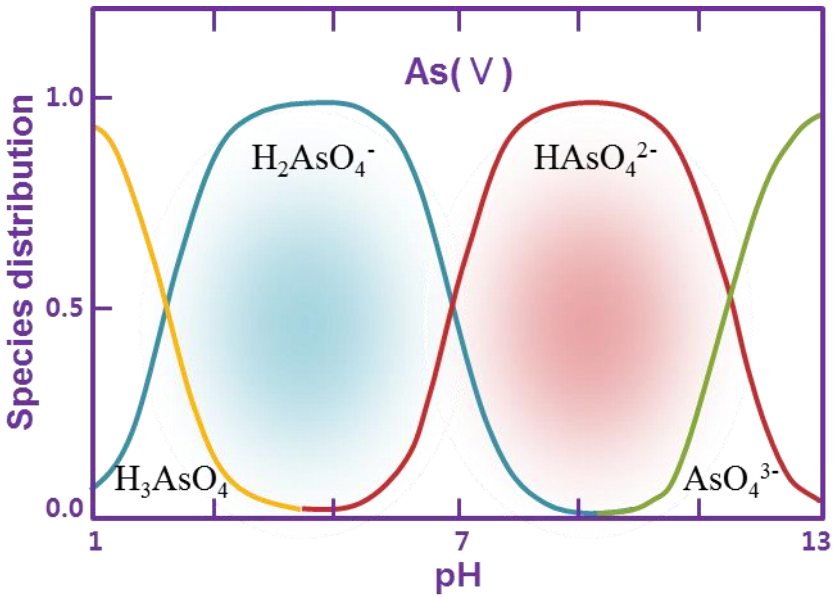

Figure 30. Occurrence of As(V) with changing pH

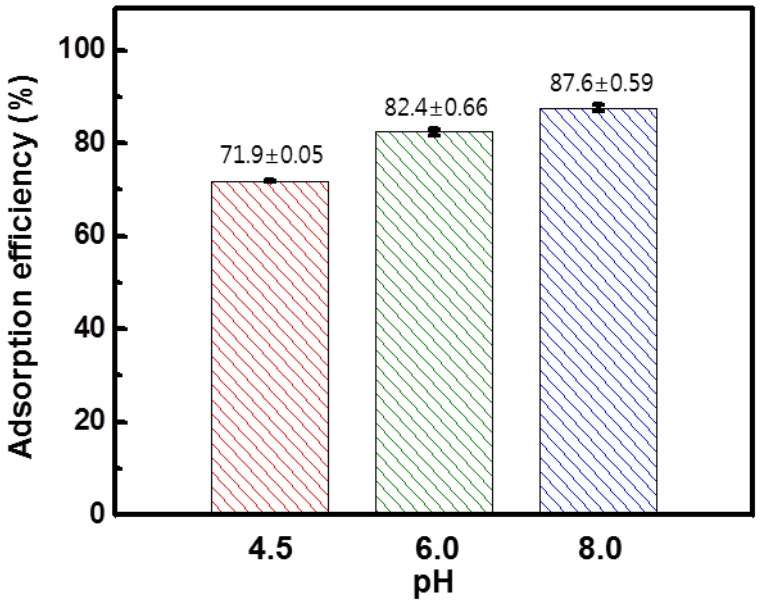

Figure 31. Maximum adsorption efficiency of QP-MG toward As(V) at various pH

3.4.3. Recovery property toward As(V)

The regeneration ability of spent adsorbent material is an important criterion when it comes to cost effective and preventing secondary contaminations. For practical applications, reusable adsorbents are economically necessary. Therefore, we found out conditions of desorption to recovery the adsorbent efficiently in water treatment process.

A large number of researchers to desorb the adsorbed As(V) from surface of adsorbents have been carried out in acidic or alkaline conditions by varying concentrations of HCl, H_2SO_4, $NaHCO_3$, Na_2CO_3 and NaOH [27].

In the present work desorption studies were conducted using two different eluents: HCl and NaOH solution and the results for recovery efficiency is shown in Figure 32. The pH for desorption the As(V) was adjusted to 2.0 and 12.3, respectively, using the 0.1 N HCl and 0.1 N NaOH. To optimize the conditions for efficient desorption of As(V), the same adsorbent was used to four sequential adsorption-desorption cycle. The results of these studies (see Figure 32) depict that recovery efficiency using the HCl solution was lower compared to the NaOH solution. The recovery efficiency is from 62.4% to 16.3% for 4 recycling test. It was observed that the solution of 0.1 N NaOH was the most suitable to adsorption-desorption systems (see Figure 3b).

We may explain that the efficiency of desorption with sodium hydroxide is ion exchanging. At higher pH, hydroxide ions of the solution are increased and compete with arsenate anions. As this time, adsorbents interact with hydroxide ions faster than arsenate ions, inducing the desorption of the adsorbed As(V) on the QP-MG. Thus, probability of desorption could be increased in alkaline conditions, resulting that recovery efficiency was higher than acidic conditions in 4 recycling test.

In contrast of alkaline conditions, the degree of desorption at lower pH could be decreased. At acidic conditions, increasing of hydrogen ions, the positive charged quaternary ammonium groups in QP-MG repel the H^+. Thus, desorption of the adsorbed As(V) in acidic conditions having the number of H^+ doesn't work well, resulting that the recovery efficiency of 45.5% at first cycle was decreased in 15.1% after 4 recycling process. The results suggest that the conditions of desorption using 0.1 N NaOH solution were suitable for efficient recovery of the As(V).

The recovery property was evaluated at alkaline conditions using identical sample performed the adsorption test at various pH. We suppose that discrepancy of strength of the interaction between QP-MG and As(V) affects the recovery efficiency due to diverse formation of the arsenate at various pH in aqueous solution. This characteristic of the arsenate that $HAsO_4^{2-}$ may interact

better than $H_2AsO_4^-$ with adsorbents would affect the recovery efficiency. The result for evaluation of the recovery property is shown in Figure 33. The recovery efficiencies were from 89.5% to 68.0%, from 84.4% to 48.7% and from 62.4% to 16.3% at pH 4.5, 6.0 and 8.0 for 4 recycling test. Most of the recovery efficiencies were decreased as increasing the pH value from 4.5 and 8.0.

Dominant species of the As(V) are changed at various pH, and result discrepancy of strength of interaction between QP-MG and As(V) in Figure 34. At acidic conditions (pH 4.5), species of $H_2AsO_4^-$ is dominant and interacts mainly with QP-MG. The species of $HAsO_4^{2-}$ is dominant and interacts mainly with adsorbents at alkaline conditions (pH 8.0). The strong interaction of $HAsO_4^{2-}$ with adsorbents at pH 8.0 decreases the recovery efficiencies because of difficulty in desorbing of the adsorbed As(V) on the QP-MG. So the recovery efficiency of 62.4% at pH 8.0 didn’t retain during 4 recycle test, and end terminated in 16.4%. In contrast of at pH 4.5, the recovery efficiency of 89.5% was maintained during recycling test, and end up terminated in 68.0%. Thus, high recovery efficiency of more than 68% was retained at pH 4.5 for recycling test. As seen from the Table 10, volume of uptake for recovery capacities of the As(V), was calculated at pH 4.5, 6.0 and 8.0 by equation:

$$q = \frac{(C_e - C_i) \times \mathrm{V}}{m}$$

,where C_e is equilibrium metal concentration (mg/L), C_i is initial metal concentration (mg/L), V is volume of metal solution (L) and m is mass of adsorbents (g).

The volume of total uptake was 27.2 mg/g, 24.5 mg/g and 14.3 mg/g at pH 4.5, 6.0 and 8.0. Thus, at pH 4.5 could be feasible for conditions to adsorb and recover efficiently toward As(V). The result suggest that the strength discrepancy of interaction of the arsenate anions with QP-MG at various pH affect not only adsorption efficiency and but also recovery efficiency. At pH 4.5 could be the most feasible conditions for adsorption and recovery of the As(V).

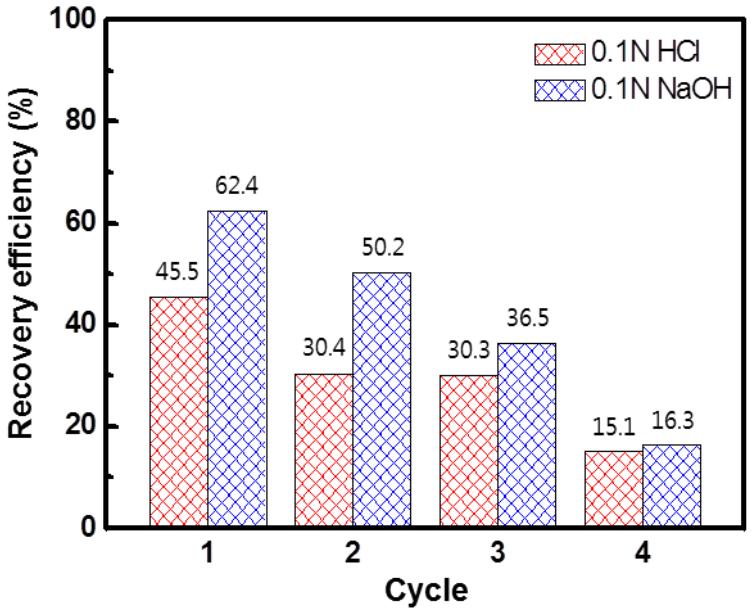

Figure 32. Recovery efficiency of QP-MG toward As(V) by 0.1 N NaOH and HCl solution, after 4 recycle test

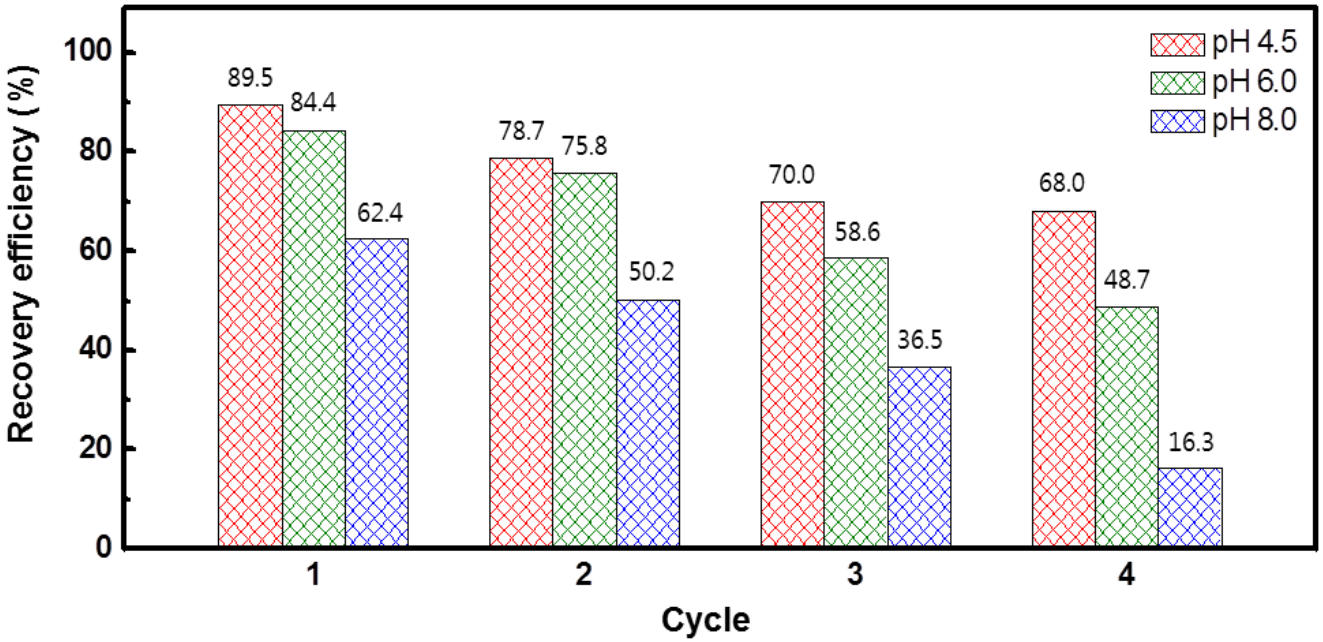

Figure 33. Recovery efficiency of QP-MG toward As(V) at pH 4.5, 6.0 and 8.0

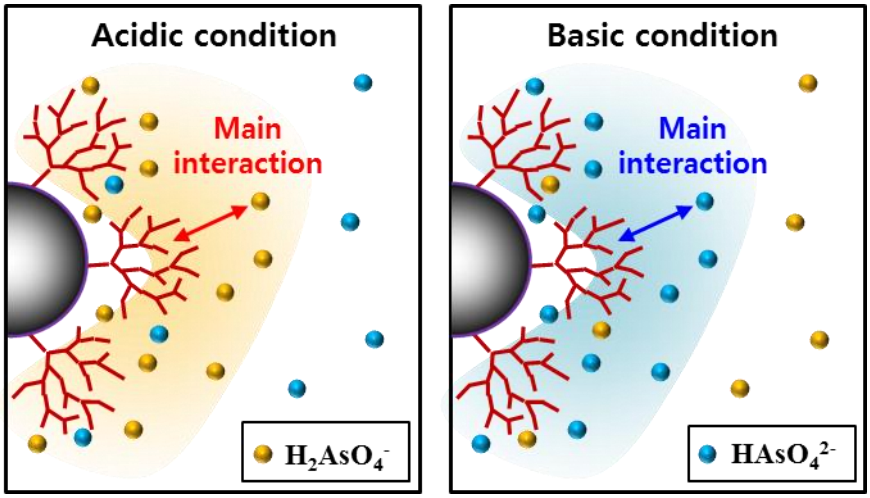

Figure 34. Interactions between QP-MG and arsenate at acidic and basic conditions

pH	4.5		6.0		8.0	
Cycle	uptake (mg/g)	*R(%)	uptake (mg/g)	R(%)	uptake (mg/g)	R(%)
1	7.94	89.5	7.84	84.4	5.38	62.4
2	6.99	78.7	7.04	75.8	4.32	50.2
3	6.21	70.0	5.45	58.6	3.15	36.5
4	6.04	68.0	4.17	48.7	1.41	16.3
total uptake	27.2 mg/g		24.5 mg/g		14.3 mg/g	

Table 10.Total adsorption capacity of QP-MG toward As(V), after 4 cycle test

3.4.4. Adsorption and recovery property toward Cr(VI)

At pH 4.5 was the most feasible conditions for adsorption and recovery of the As(V). This result could be applied to remove the other anionic heavy metals such as a chromium (Cr(VI)). Thus, we studied to investigate for maximum adsorption efficiency toward Cr(VI) at pH 4.5.

The Cr(VI) is dependent with pH conditions in aqueous system such as a As(V) and most of Cr(VI) exist one-electron negative anions ($HCrO_4^-$) at pH 4.5. Most of the chromium anions at pH 4.5 exists $HCrO_4^-$ and it may be interact with adsorbents by electrostatic attraction. The results of adsorption and recovery experiments toward Cr(VI) are shown in Figure 35a,b. The A% at pH 4.5 was presented 79.6% and R% of more than 96% was terminated in 52.2%, after 4 recycle test. High R% of more than 52.2% at pH 4.5 toward Cr(VI) was maintained during 4 recycle test.

Equilibrium isotherm governing the maximum adsorption capacity is one of the important characteristics that define the adsorption efficiency.

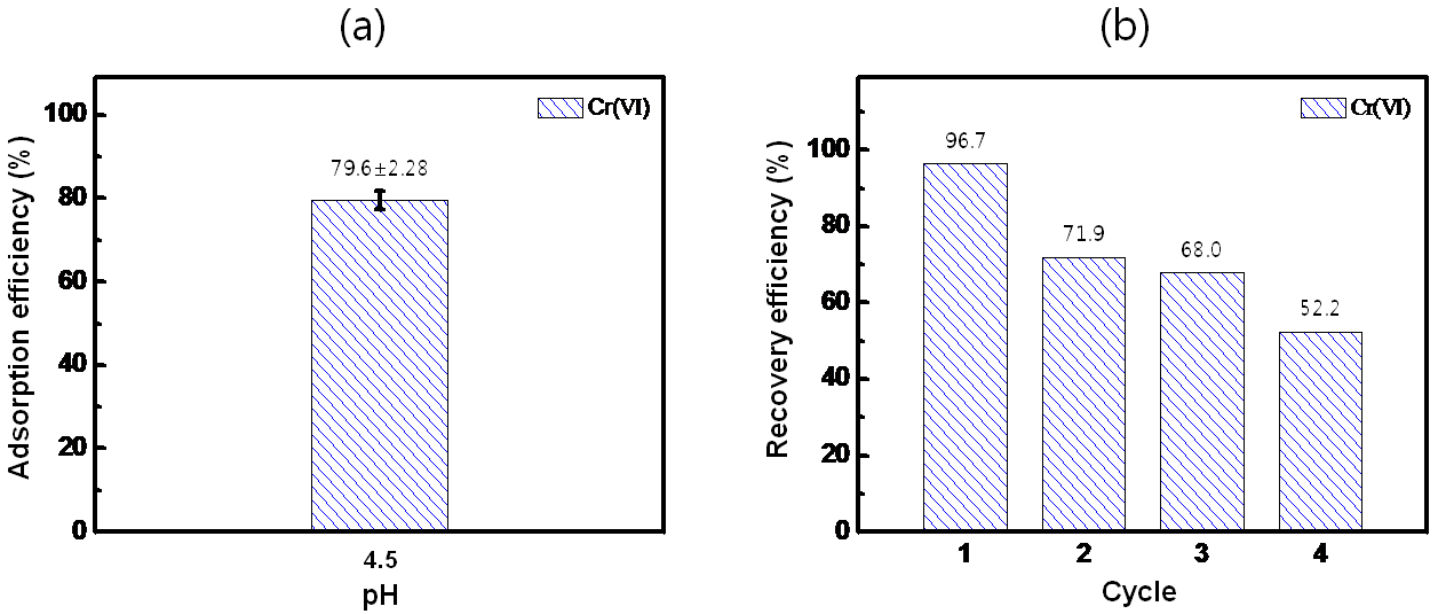

Figure 35. (a) Adsorption efficiency of QP-MG toward Cr(VI) at pH 4.5 (b) Recovery efficiency for 4 cycle toward Cr(VI) at pH 4.5

3.4.5. Equilibrium isotherm

Equilibrium isotherm governing the maximum adsorption capacity is one of the important characteristics that define the adsorption efficiency. Experiment for calculation of the maximum capacity carried out in arsenate solutions (50 mL) containing $Na_2HAsO_4 \cdot 7H_2O$ (10, 50, 100, 200 and 400 mg). These results are shown in Figure 36 and Table 11.

Langmuir equation was used to describe the equilibrium characteristics of adsorption among these equations such as a Freundlich, Redlich-Peterson and Langmuir-Freundlich equation, etc. The adsorption capacities of the as-obtained QP-MG toward As(V) and Cr(VI) were measured at pH 4.5, which may be feasible conditions for adsorption and recovery system. The results with corresponding, Langmuir plot were presented in Figure 36 inset.

<Langmuir equation>

$$q_e = \frac{q_m b C_e}{(1 + bC_e)}$$

$$\frac{1}{q_e} = \frac{1}{bq_m} C_e + \frac{1}{q_m}$$

The fitted constants along with regression coefficients (R^2) are summarized in Table 11. The data of the As(V) and Cr(VI) adsorbed at equilibrium (q_e, mg/g) and equilibrium concentration (C_e, mg/L) were fitted to the Langmuir adsorption model. The data was fitted well to the model with correlation coefficients (R^2) of 0.9909 and 0.9739.

Therefore, the adsorption of heavy metal ions onto QP-MG occurs in monolayer and surface of the adsorbents is homogeneous. As listed in Table 11, the calculated maximum adsorption capacity of As(V) and Cr(VI) were 20.9 mg/g and 23.5 mg/g.

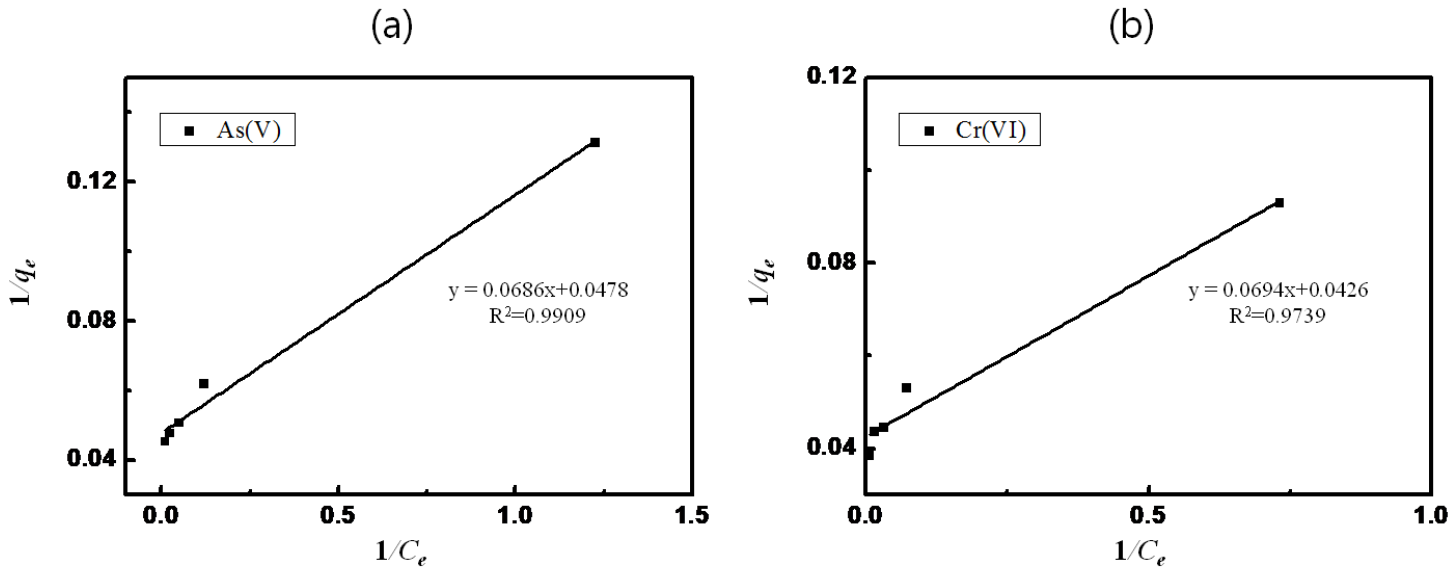

Figure 36. (a) Langmuir results of QP-MG toward As(V) (b) Langmuir results of QP-MG toward Cr(VI) for calculation of the maximum adsorption capacity at pH 4.5

Langmuir constant	As(V)	Cr(VI)
q_m	20.9	23.5
b	3.282×10^{-3}	2.9531×10^{-3}
R^2	0.9909	0.9739

Table 11. Langmuir constants of QP-MG toward As(V) and Cr(VI)

4. Conclusion

In the present study, the branched polyethylenimine containing a number of amine functional groups were incorporated to magnetite particles. We were synthesized polyethylenimine-functionalized magnetite (P-MG) and quaternary ammonium polyethylenimine-functionalized magnetite (QP-MG) with the aim of discussing; evaluation for feasibility of adsorbents to remove heavy metal ions from contaminated water and the reusability of the adsorbents. The conclusions obtained from this study are as follows.

1. Branched polyethylenimine (b-PEI) has amine-rich structure and highly branched structure with positive charge density, making it important that adsorbents chelate heavy metal ions and are feasible modified by various functional groups. Modified adsorbents by b-PEI were applied to remove the heavy metals. Amine-functionalized magnetite (AMG) was applied for development of reusable adsorbents for efficient separation in external magnetic field. Degree of branching and existence of the amine groups in b-PEI were confirmed using C^{13} NMR and FT-IR. Magnetic characteristics of AMG were analyzed using VSM, resulting that AMG had paramagnetic and

high magnetization of 82.3 emu/g.

2. Polyethylenimine-functionalized magnetite (P-MG) was synthesized by surface modification of AMG using cyanuric chloride as linking agents for introduction of branched polyethylenimine (b-PEI) on surface of the AMG. After modification, we confirmed that crystal structure and morphology of the P-MG were maintained spinel structures of the spherical magnetite by XRD, HR-TEM and FE-SEM. Magnetization and paramagnetic characteristics of the P-MG were sufficient for separation and recovery of the adsorbents from aqueous solution (VSM analysis). The qualitative and quantitative evidence of surface modification by the b-PEI was derived from FT-IR, EA, XPS and TGA. The XPS analysis showed that increased signal 398.7 eV may be attributed by amine groups of the b-PEI. Through the result of TGA, we confirmed that about 3.87% of b-PEI was introduced in P-MG.

3. Quaternary ammonium polyethylenimine-functionalized magnetite (QP-MG) was synthesized by quaternization of the P-MG using glycidyltrimethylammonium chloride (GTA). After quaternization, we validated using HR-TEM and VSM that surface of the QP-MG were covered with organic materials such as a polymer and then result in a little reduction

of its magnetization in contrast of the AMG. But, spinel structure, spherical shape and magnetic characteristics of the QP-MG were maintained during modification procedures. The evidence of surface modification by the GTA was derived from FT-IR, XPS and TGA qualitatively and quantitatively. FT-IR analysis showed that formation of $C\text{-}N^{+}$ peak (1480 cm^{-1}) would be attributed by quaternary ammonium groups of quaternary ammonium polyethylenimine. Moreover, we confirmed by XPS that shifting the peak of N 1*s* in P-MG to higher biding energy is attributed by introduction of quaternary ammonium groups using GTA.

4. Adsorption mechanism of P-MG with b-PEI is explained that amine groups of P-MG could chelate with Cu(II) and Pb(II)at alkaline conditions and release by repulsion of protonated amine groups with positive charged metal ions. To find out adsorption conditions for the highest removal property of the adsorbents, adsorption efficiency are measured at various pH, resulting that that maximum adsorption efficiency of 96% and 97% were measured at pH 8.0 toward Cu(II) and Pb(II). The recovery efficiencies were shown of more than 94%, after 4 cycling test.

5. Adsorption mechanism of QP-MG with positive charged functional group is explained that interaction between quaternary ammonium groups of adsorbents and arsenate anions. The adsorbents and arsenate bind through ionic-bond and electrostatic interaction at various pH value (4.5, 6.0 and 8.0) and release the adsorbed As(V) from surface on the adsorbents through the ion exchanging by hydroxide ions. Discrepancy of strength of interaction between QP-MG and As(V) forming $H_2AsO_4^-$ and $HAsO_4^{2-}$ at various pH value in aqueous solution may affect adsorption and recovery efficiency. The highest adsorption efficiency of 87% was presented at pH 8.0 because of strong interaction between $HAsO_4^{2-}$ and QP-MG. At pH 4.5, most of As(V) exists $H_2AsO_4^-$ in water, making it important that the recovery efficiency of more than 68% was maintained, after 4 recycling test. Thus, pH 4.5 could be feasible for adsorption conditions to effective regenerate the adsorbents.

6. The condition of the pH 4.5 was applied to adsorption and recovery experiments for Cr(VI). Cr(VI) exist as oxyanions at various pH in aqueous systems like As(V). The adsorption efficiency of 71% was presented at pH 4.5, which is the condition containing dominant species of $HCrO_4^-$. Recovery efficiency of more than 52% was maintained, after 4 recycle test.

7. Equilibrium isotherm governing adsorption reaction is one of the important characteristics that define the maximum adsorption capacity. The equilibrium characteristics of adsorption have been used to describe with Langmuir model. Maximum adsorption capacity of the P-MG and QP-MG toward heavy metal ions were calculated using Langmuir equation. The Langmuir plot corresponding with Cu(II), Pb(II), As(V) and Cr(VI) were presented and the data was fitted well to the Langmuir model with R^2 of more than 0.9. The maximum adsorption capacity of P-MG and QP-MG was 158.7 mg/g, 163.9 mg/g, 20.9 mg/g and 23.5 mg/g toward Cu(II), Pb(II), As(V) and Cr(VI).

Consequently, P-MG was successfully synthesized using b-PEI including a number of amine groups chelating with heavy metals. The QP-MG with quaternary ammonium group that interacts with arsenate and chromium was obtained through the modification by GTA. These adsorbents were applied for removal and recovery of heavy metal ions from contaminated water. Through the results that P-MG was shown high adsorption and recovery efficiencies toward Cu(II) and Pb(II), and QP-MG was feasible for recovery of As(V) and Cr(VI) at pH 4.5, we confirmed that prepared adsorbents would be promising candidates for efficient removal and recovery of heavy metal ions.

5. Reference

[1] Y.C. Lee, W.K. Park, J.W. Yang, Removal of anionic metals by amino-organoclay for water treatment, J. Hazard. Mater. 190 (2011) 652-658

[2] S. Singh, K.C. Barick, D. Bahadur, Surface engineered magnetic nanoparticles for removal of toxic metal ions and bacterial pathogens, J. Hazard. Mater. 192 (2011) 1539-1547

[3] F. Fu, Q. Wang, Removal of heavy metal ions from wastewaters: A review, J. Environ. Manage. 92 (2011) 407-418

[4] R. Naseem, S.S. Tahir, Removal of Pb(II) from aqueous solution by using bentonite as an adsorbent, Water Res. 35 (2001) 3982-3986

[5] I.Y. Goon, C. Zhang, M. Lim, J.J. Gooding, R. Amal, Controlled fabrication of polyethylenimine-functionalized magnetic nanoparticles for the sequestration and quantification of free Cu^{2+}, Langmuir 26(14) (2010) 12247-12252

[6] W. Jiang, X. Chen, Y. Niu, B. Pan, Spherical polystyrene-supported nano-Fe_3O_4 of high capacity and low-field separation for arsenate removal from water, J. Hazard. Mater. 243 (2012) 319-325

[7] S.W. Al. Rmalli, C.F. Harrington, M. Ayub, A biomaterial based approach for arsenic removal from water, J. Environ. Monit. 7 (2005) 279-282

[8] J. Pattanayak, K. Mondal, S. Mathew, S.B. Lalvani, A parametric evaluation of the removal of As(V) and As(III) by carbon-based adsorbents, Carbon 38 (2000) 589-596

[9] J. Zhang, T. Ding, C. Zhang, Biosorption and toxicity responses to arsenite (As[III]) in scenedesmus quadricauda, Chemosphere 92 (2013) 1077-1084

[10] X.F. Sun, Y. Ma, X.W. Liu, S.G. Wang, B.Y. Gao, X.M. Li, Sorption and detoxification of chromium(VI) by aerobic granules functionalized with polyethylenimine, Water Res. 44 (2010) 2517-2524

[11] J. Sanchez, B.L. Rivas, Cationic hydrophilic polymers coupled to ultrafiltration membranes to remove chromium (VI) from aqueous solution, Desalination 279 (2011) 338-343

[12] G. Wojcik, V. Neagu, I. Bunia, Sorption studies of chromium(VI) onto new ion exchanger with tertiary amine, quaternary ammonium and ketone groups, J. Hazard. Mater. 190 (2011) 544-552

[13] L.K. Wang, Y.T. Hung, N.K. Shammas, Advanced physicochemical treatment technologies, In: Handbook of Environmental Engineering vol.5 Humana, Newjersey

[14] X. Xin, Q. Wei, J. Yang, R. Feng, G. Chen, Highly efficient removal of heavy metal ions by amine-functionalized mesoporous Fe_3O_4 nanoparticles, Chem. Eng. J. 184 (2012) 132-140

[15] M. Neu, D. Fischer, T. Kissel, Recent advances in rational gene transfer vector design based on poly (ethylene imine) and its derivatives, J. Gene. Med. 7 (2005) 992-1009

[16] M. Jager, S. Schubert, S. Ochrimenko, Branched and linear poly (ethylene imine)-based conjugates: synthetic modification, characterization, and application, Chem. Soc. Rev. 41 (2012) 4755-4767

[17] S. Deng, Y.P. Ting, Polyethylenimine-modified fungal biomass as a high-capacity biosorbent for Cr (VI) anions: sorption capacity and uptake mechanisms, Environ. Sci. Technol. 39 (2005) 8490-8496

[18] Y. Pang, G. Zeng, L. Tang, Y. Zhang Y. Liu, X. Lei, Z. Li, PEI-grafted magnetic porous powder for highly effective adsorption of heavy metal ions, Desalination 281 (2011) 278-284

[19] J. Liu, S. Ma, L. Zang, Preparation and characterization of ammonium-functionalized silica nanoparticle as a new adsorbent to remove methyl orange from aqueous solution, Appl. Surf. Sci. 265 (2013) 393-398

[20] K. Mandel, F. Hutter, C. Gellermann, Modified superparamagnetic nanocomposite microparticles for highly selective Hg(II) or Cu(II) separation and recovery from aqueous solutions, ACS Appl. Mater. Interfaces 4 (2012) 5633-5642

[21] L. Wang, J. Bao, L. Wang, F. Zhang, One-pot synthesis and bioapplication of amine-functionalized magnetite nanoparticles and hollow nanospheres, Che. Eur. J. 12 (2006) 6341-6347

[22] T. Qiang, M. Luo, Q. Bu, X. Wang, Adsorption of an acid dye on hyperbranched aminated collagen fibers, Chem. Eng. J. 197 (2012) 343-349

[23] K. Khunathai, D. Parajuli, K. Ohto, Adsorption behavior of quaternary amine types of lignophenol compounds for some precious metals, SolventExtr. Ion. Exc. 28 (2010) 403-414

[24] M. Seiler, Hyperbranched polymers: phase behavior and new applications in the field of chemical engineering, Fluid phase Equailibr. 241 (2006) 155-174

[25] B. Xiao, X. Wang, Z. Qiu, J. Ma, L. Zhou, A dual-functionally modified chitosan derivative for efficient liver-targeted gene delivery, J. Biomed. Mater. Res. A 101A (2013) 1888-1897

[26] C.W. Nam, Y.H. Kim, S.W. Ko, Modification of polyacrylonitrile (PAN) fiber by blending with N-(2-hydroxy) propyl-3-trimethyl-ammonium chitosan chloride, J. Appl. Polym. Sci. 74 (1999) 2258-2265

[27] S. Saha, P. Sarkar, Arsenic remediation from drinking water by synthesized nano-alumina dispersed in chitosan-grafted polyacrylamide, J. Hazard. Mater. 227-228 (2012) 68-78

국문 초록

전지, 페인트, 프린트, 자동차, 합금 등의 생산 및 제조산업에서 중금속의 사용량이 늘어남에 따라, 중금속의 유출에 의한 인간의 피해 및 환경오염 문제가 급격하게 증가하고 있다. 중금속의 일부는 필수원소로 인간의 생체 내 대사에 필수적인 역할을 하지만, 대부분의 중금속은 수 중에 해리되어 이온상태로 존재하며, 생체 내에서 분해되지 않고 축적되는 특징을 갖는다. 즉, 극소량만으로도 먹이사슬에 의해 중금속이 체내에 축적되어 최종소비자인 인간에게 다양한 질병을 유발할 뿐만 아니라 생태계를 파괴한다. 따라서 수중에 존재하는 중금속을 효과적으로 제거하면서도, 재사용이 가능한 흡착제에 대한 연구가 필요하다고 생각하였다.

이 연구에서는 **가지구조형 폴리에틸렌이민(branched polyethylenimine, b-PEI)**가 도입된 **자성입자**를 이용하여 **구리, 납, 비소, 크롬**과 같은 중금속 이온을 제거할 수 있는 재사용이 가능한 흡착제를 개발하고자 하였다. 가지구조형 고분자인 **b-PEI는 중금속을 효과적으로 킬레이팅** 할 수 있는 고분자로 잘 알려져 있으며, 이러한 아민구조는 정전기적 인력을 통해 양이온 금속이온과 결합할 수 있으며, 흡착된 금속이온은 수소화된 아민구조와의 반발력에 의해 다시 효과적으로 방출될 수 있다. **4차 암모늄기로 개질된 b-PEI** 또한

이온결합에 의해 **음이온 금속과 결합**할 수 있으며, 흡착된 이온은 이온교환을 통해 다시 방출될 수 있다. 외부자기장 하에서 효과적으로 분리·회수 할 수 있는 자성입자인 마그네타이트의 장점을 수질 정화 과정에 적용하고자 하였다.

양이온 형태의 중금속인 구리, 납을 제거하기 위하여 b-PEI가 도입된 자성입자(P-MG)를 합성하였다. 아민기가 활성화된 자성입자(AMG) 표면에 (cyanuric chloride)와 같은 가교제를 이용하여 b-PEI를 도입하였다. 또한 음이온 형태의 비소와 크롬을 제거하기 위하여 (glycidyltrimethylammonium chloride, GTA)를 이용하여 4차 암모늄기로 개질된 b-PEI가 도입된 자성입자(QP-MG)를 합성하였다.

b-PEI와 GTA에 의한 정성·정량적 분석을 위해 적외선 분광분석(FT-IR), X선 광전자분광분석(XPS), 열중량 분석(TGA)을 실시하였으며, 이를 통해 b-PEI와 4차 암모늄기를 갖는 b-PEI가 자성입자에 잘 도입이 되었다는 것을 확인하였다. X선 광전자회절분석법(WXRD), 전계방출주사전자현미경(FE-SEM), 고분해능 투과전자현미경(TEM)를 이용하여 합성된 흡착제의 결정구조와 모폴로지(morphology)를 분석하였고, 고분자와 같은 유기물질이 흡착제의 표면에 쌓인 것을 관찰할 수 있었다. P-MG와 QP-MG 모두 스피넬 구조를 갖는 구형의 자성입자 형태를 유지하고 있는 것을 확인하였으며, 이를 통해 b-PEI와 GTA에 의한 개질이 흡착제의 결정구조 및 모폴로지

(morphology)에 어떠한 영향을 주지 않는다는 것을 알 수 있었다. 또한 (vibrating sample magnetometry, VSM)을 이용한 자력분석을 통해 P-MG, QP-MG 모두 수중에서 분리하기에 충분한 **자력**을 가진 AMG와 유사한 자력 측정값을 가지며, 이는 **수중에서 반복적으로 분리·회수하여 사용**될 수 있을 것으로 기대된다.

구리, 납, 비소에 대한 흡착 및 재사용 성능을 최적화 하기 위해, 다양한 pH조건에서 흡착 및 방출 실험을 수행하였다. 그 결과, P-MG는 구리와 납에 대하여 각각 **96%, 97%의 최대 흡착효율**을 나타내었습니다. 더불어 4회의 재사용 성능 평가에서도 **구리와 납 모두에 대하여 94% 이상의 높은 재사용 효율**을 갖는 것을 확인하였습니다. 특히 QP-MG의 흡착 및 재사용 성능은 pH환경에 따라 수중에서 다양한 형태로 존재하는 비소에 의해 많은 영향을 받는 것을 알 수 있었다. 실험 결과, QP-MG는 비소의 대부분이 $HAsO_4^{2-}$로 존재하는 **pH 8.0에서 87%의 가장 높은 흡착효율**을 보였다. 이는 비소의 대부분이 -2 형태의 이온으로 존재하는 pH 8.0에서 흡착제와 이온결합을 통해 -1가 형태의 이온보다 더 강하게 결합함으로써 가장 높은 흡착효율을 나타낸 것으로 생각된다. 이와 반대로, 비소의 대부분이 -1가 형태로 존재하는 **pH 4.5에서 68%이상의 가장 높은 재사용 효율**을 가지는 것을 확인할 수 있었다. 또한 비소와 같이 수중에서 음이온 형태로 존재하는 크롬에 대하여 pH 4.5에서 흡착 및 재사용 평가 실험을 진행하였다. 그 결

과, 동일한 pH조건에서 **71% 이상의 흡착효율과 52% 이상의 재사용 효율**을 갖는 것을 알 수 있었다.

Langmuir 모델을 적용함으로써 구리, 납, 비소, 크롬 각 이온에 대하여 흡착제 1 g 당 각각 **18.7 mg, 163.9 mg, 20.9 mg, 23.5 mg의 최대흡착량**을 갖는 알 수 있었다. 또한 4회의 재사용 성능평가를 통해 흡착제의 재사용 효율이 잘 유지되는 것을 확인 할 수 있었다. 위의 실험결과를 통해, P-MG와 QP-MG가 구리, 납, 비소, 크롬이온에 대하여 높은 흡착 효율을 갖는 재사용이 가능한 흡착제로써의 가능성을 확인할 수 있었다.

결론적으로 b-PEI가 도입된 자성입자를 포함하는 흡착제를 성공적으로 합성하였으며, 수중에 존재하는 중금속이온을 효과적으로 제거하면서도 재사용이 가능한 흡착제로 적용하였다. 이는 **중금속 제거를 위한 재사용이 가능한 수처리 재료**로 다양하게 효과적으로 사용될 것을 기대한다.

감사의 글

길고도 짧았던 2 년간의 석사과정을 마치고 또 다른 미래를 위해 도약하고자 합니다. 먼저 무사히 석사과정을 마치고 졸업할 수 있도록 많은 가르침을 주신 모든 분들께 감사의 마음을 전합니다. 2 년 동안 많은 관심과 격려로 지도해주신 곽승엽 교수님께 깊은 감사를 드리며 바쁘신 와중에도 졸업 논문을 심사해주시고 지도해 주신 장지영 교수님과 안철희 교수님께 진심으로 감사 드립니다. 2 년간의 석사과정을 뒤돌아보면 힘들고 어려울 때도 많았지만, 앞으로 다가올 미래에 있을 어려움을 해결해 나가는 든든한 기반이 되어줄 많은 경험과 지식을 쌓을 수 있었던 값진 시간이었습니다. 늘 함께 고민해주고 옆에서 격려와 조언을 아끼지 않았던 실험실 동료들이 있었기 때문에 석사졸업이라는 큰 결실을 맺을 수 있었다고 생각하며, 진심으로 감사의 마음을 전합니다. 제일 먼저, 바쁘신 와중에도 직접 오셔서 매번 연구에 대한 열정과 관심으로 지도해 주신 정재우 교수님, 나이에 상관없이 모든 연구실 식구들을 포용할 수 있는 넓은 마음과 센스를 지니신 최성학 선배님, 전지에 대해 아무것도 몰랐던 제게 자상하게 도움을 주신 전재덕 박사님께도 매우 감사 드립니다. 졸업 직전에도 연구적으로 많은 도움주신 닮고 싶은 병용 선배님, 입학부터 졸업까지 든든한 대장역할을 해주신 수열 선배님, 날카로운 지적으로 부족한 것을 채울 수 있게 해주신 형구 선배님, 남자만 있는 실험실에서 적응할 수 있도록 배려해 주시고 늘 유쾌한 장난으로 연구실에 활력소가 되어주신 현중 선배님, 하나부터 열까지 챙겨주시고 섬세한 조언으로 연구에 많은 도움을 주신 성용 선배님, 처음부터 끝까지 올바른 방향으로 나아갈 수 있게 나침반 같은 역할을 해주신 우혁 선배님, 하나뿐인 사수로서 좋은 본보기가 되어주신 범진 선배님, 덤벙대는 저를 친오빠처럼 자상하게 챙겨주신 지훈 선배님, 실험실에서 일어나는 모든 일에 척척박사라 많이 배웠던 지환 선배님, 여자인 저보다 더 소녀적인 감성으로 따뜻하게 조언해주신 태선 선배님, 조용하지만 강하게 꼭 필요한 조언을 해주셔서 늘 감사했던 효원 선배님, 긴 시간 동안 변함없이 누구보다 힘이 되어준 규원 선배님, 여유롭게 잘 해내는 동기 준호, 오랜 기간 동안 실험실의 궂은일 하느라 고생해 준 든든한 후배 승희 오빠, 칙칙한 실험실에 비타민 같은 활력을 불어넣어준 여성스러운 후배 예지까지, 연구실 모든 선·후배님들께 진심으로 감사의 마음을 전합니다. 마지막으로 믿음과 사랑으로 지지해주신 부모님, 하나뿐인 내 동생 민주와 즐겁고 힘들었던 모든 추억에 함께였고 앞으로도 함께할 소중한 친구들에게도 감사의 마음을 전하며 앞으로도 계속 발전하는 모습을 보여주기 위해 노력할 것을 약속합니다.